YNTHESIS OF INTERNALLY LINKED CARBAZOLE DNA OLIGOMERS: A POTENTIAL MONITOR FOR CHARGE TRANSFER IN DNA STUDIES

A Thesis
Presented to
The Academic Faculty

By

Chiko Umeweni

In Partial Fulfillment
of the Requirements for the Degree
Master of Science in the
School of Chemistry and Biochemistry

Georgia Institute of Technology
August, 2005

SYNTHESIS OF INTERNALLY LINKED CARBAZOLE DNA OLIGOMERS: A POTENTIAL MONITOR FOR CHARGE TRANSFER IN DNA STUDIES

Approved by:

Dr. Gary B Schuster, Chair
School of Chemistry and Biochemistry
Georgia Institute of Technology

Dr. David Collard
School of Chemistry and Biochemistry
Georgia Institute of Technology

Dr. Christoph J. Fahrni
School of Chemistry and Biochemistry
Georgia Institute of Technology

Date Approved: July 18, 2005

For my parents and siblings. Thank you for all your support.

ACKNOWLEDEMENTS

I would like to extend a big thank you to my advisor Dr. Gary B. Schuster for his support, advice and guidance during my time in his research group. I have learned much from you and hope to go on and influence others as you have done me. I would like to thank my committee members for their kind words and encouragement. Special thanks go to Dr. Marcus Weck who believed in my inner potential when I didn't.

I would also like to thank the post docs in the Schuster group. Abraham, Sriram, Rick, Bhaskar, Joshy and Chucheng, thank you for teaching me virtually everything I know about synthesis in the real world. As for the graduate students of Schuster group, where do I begin to express my appreciation for the kindness and support you bestowed upon me? Lezah, Thabi, Gozde, Nate, Frank, Prolay and Avik, this experience would not have been the same without you guys. Extra thanks go to the two best friends one could possibly ask for Gozde and Christy. What would I do without you two?

Finally, I reserve my last and most humble thanks for my family without whom I would be truly lost.

TABLE OF CONTENTS

LIST OF FIGURES AND TABLES

LIST OF SCHEMES

LIST OF ABBREVIATIONS AND SYMBOLS

A	Adenine
AQ	Anthraquinone
C	Cytosine
CD	Circular Dichroism
CZ	Carbazole
DNA	Deoxyribonucleic Acid
G	Guanine
HPLC	High Performance Liquid Chromatography
MS	Mass Spectrometry
NMR	Nuclear Magnetic Resonance Spectroscopy
ODN	Oligonucleotide
PAGE	Polyacrylamide Gel Electrophoresis
SCE	Standard Calomel Electrode
T	Thymine
Tm	Melting Temperature
TQ	Tetracene Quinone (tetraquinone)
U	Uridine
UAQ	Uridine linked Anthraquinone
U1Z	1-Carbon linked Carbazole Uridine
U4Z	4-Carbon linked Carbazole Uridine
UV-Vis	Ultraviolet - Visible

SUMMARY

In duplex DNA, guanine radical cations react with water or molecular oxygen to form mainly 7,8-dihydro-8-oxoguanine (8-OxoG). Understanding of the mechanism for migration of a radical cation (hole) from the site of initial DNA oxidation to a remote guanine is an important step in the process that will lead to a thorough understanding of DNA damage and its repair.

Long distance hole transfer through DNA is usually studied by strand cleavage analysis. This requires injection of a radical cation into a ^{32}P labeled DNA strand and cleavage at the oxidized sites (usually GG steps) with a suitable agent (eg: piperidine). This is followed by analysis with polyacrilamide gel electrophoresis and quantification of damage with a phosphorimager.

Many studies have been performed to study hole transfer through DNA and the vast majority of them utilize guanine oxidation as a monitor for charge transfer. The synthesis of a potential monitor for charge transfer through DNA that is independent of guanine oxidation is reported herein. The system is a carbazole moiety covalently attached to the 2'-O of uridine which is subsequently incorporated into a DNA strand.

INTRODUCTION

DNA structure

Deoxyribonucleic acid (DNA) is a complex molecule that is found in living systems. It is the vehicle of inheritance and contains all the genetic information needed to ensure the normal development and functioning of organisms. DNA is made up of four different nucleotides with each nucleotide consisting of a nitrogenous base (adenine, guanine, cytosine or thymine), a sugar (deoxyribose) and a phosphate group (see figure 1). The nucleotides are linked to each other *via* a phosphodiester bond between the 3' –OH and 5' –OH of the neighboring sugars. Genetic information is encoded in the precise linear sequence of the nucleotides.[1]

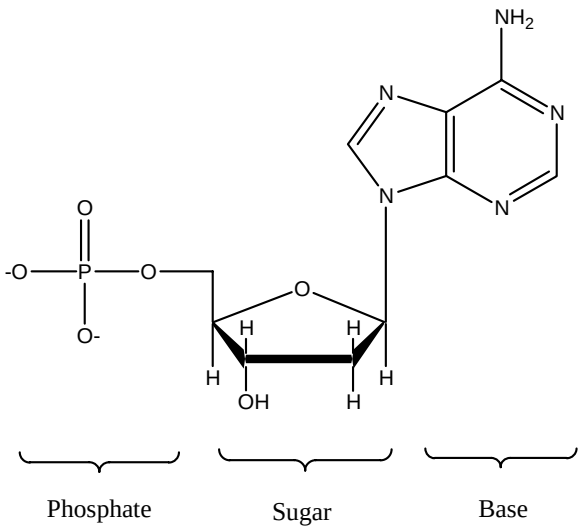

Figure 1. Structure of the nucleotide adenine

When DNA's double helix structure was determined by James Watson and Francis Crick in 1953,[2] two forms of DNA were reported: A-form and B-form. The B-form of DNA, the most common, is obtained when DNA is fully hydrated, as is the case

in vivo. A-form however is observed under dehydrated non-physiological conditions. DNA can undergo a conformational switch from B-form to A-form during replication.[3] Both A-form and B-form have the shape of a right-handed helical staircase (figure 2) with rails represented by the sugar phosphate backbone and rungs as hydrogen bonded bases. The nitrogenous bases are of two forms: purines and pyrimidines. Adenine(A) and guanine(G) are purines, while thymine(T) and cytosine(C) are pyrimidines. Adenine forms a base pair with thymine *via* hydrogen bonding while guanine pairs with cytosine (figure 3). There are two hydrogen bonds between AT base pairs while GC base pairs have three hydrogen bonds.

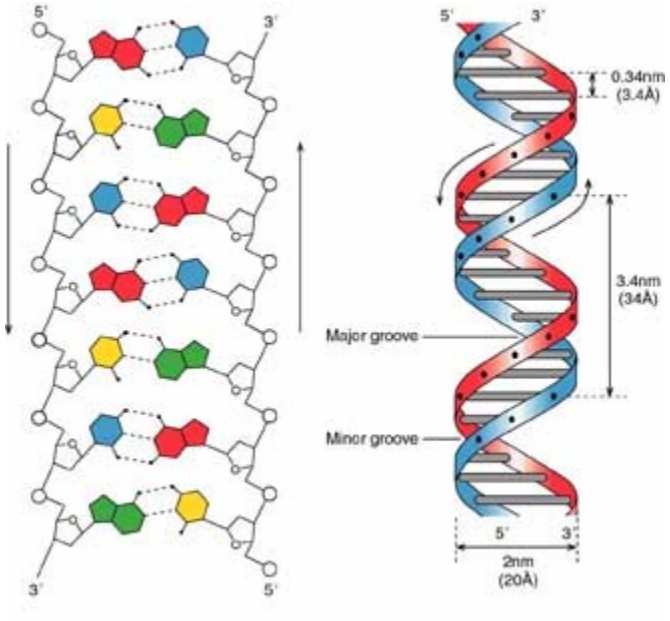

Figure 2. Helical structure of double stranded B-form DNA[4]

B-DNA has an average of 10 base pairs per turn of the helix and the space between each base pair is 3.4Å. As genetic information is encoded into the specific sequence of the nucleotide, errors in the base sequence can lead to mutant DNA and

mutant DNA can cause errors in transcription and translation which potentially leads to disease.

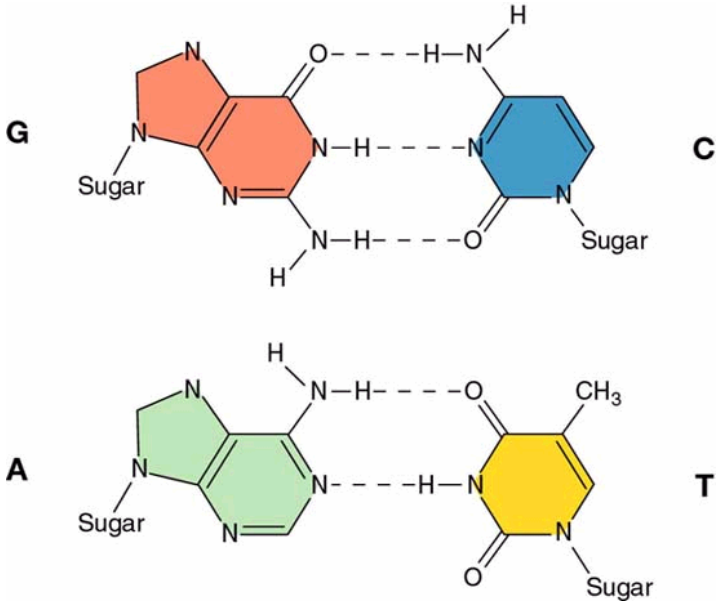

Figure 3. Hydrogen bonding between Watson-Crick base pairs

Charge transfer through DNA – Introduction

Understanding of the processes that damage DNA is of great importance as damage to DNA can lead to aging and disease, including cancer.[5] One electron oxidation of DNA creates a radical cation (hole) in DNA and upon reaction with water leads to damage in the DNA strand. The damaged sites are often far from the initial oxidation site.[6]

Extensive research has shown that long distance hole transport requires intermediate guanines (also adenines to a lesser extent) to function as temporary charge

carriers.[7, 8, 9] Owing to its low oxidation potential, guanine is the most easily oxidized base among all four bases of DNA[10] (see table 1) and its radical cation is the most stable.

Table 1. Oxidation potential of DNA bases at pH = 7 (vs SCE)[10, 11]

	Guanosine	Adenosine	Cytidine	Thymidine
E^0 (V)	1.29	1.42	1.6	1.7

The reactivity of guanine towards photo-oxidation is sequence dependent in that there is a preferential selectivity of cleavage guanines on the 5'G of 5'-GG-3' or 5'-GA-3' over all cleavage sites.[12] The base pair stacking and overlap of π electrons of DNA bases provides a path for efficient charge transfer over long distances. In fact, damage to DNA at a guanine residue as far as 200Å away from the excitation site was reported by Barton and co-workers.[7]

Charge transfer through DNA – Mechanism

A few models have been proposed to explain the mechanism of charge migration in DNA. Of these models, the two extremes are the superexchange mechanism and discrete hopping. The superexchange mechanism assumes DNA behaves like a molecular wire with delocalized molecular orbitals. Each base pair is in electronic contact with every other base pair and charge transfer occurs via superexchange. This model was supported by observation of rapid photoinduced charge transfer over 40 angstroms between metallointercalators tethered to opposing 5' – ends of a 15 base pair

DNA duplex.[13, 14] Recent work by Sen and co-workers has however shown the "wire-like" behavior of DNA model to be invalid.[15] The hopping mechanism presumes that the radical cation is localized on one base and has no significant overlap with its neighboring base pair. The migration of the radical cation through bases occurs by a thermally activated process.[16] A third mechanism "phonon-assisted polaron-like hopping" for DNA charge migration was proposed by Schuster,[9] and has since gained a lot of support[17]. This model of charge transport through DNA is based on discrete electron-transfer reactions between neighboring bases or groups of bases.

Charge transfer through DNA – Experimentation

Photosensitizers and mechanism of AQ photoexcitation

Many experimental systems have been designed to understand the mechanistic pathways for charge transfer in DNA. These systems involve introduction of a radical cation into DNA by irradiation of a light activated compound in the presence of DNA duplex. Photosensitizers such as rhodium complexes,[18] naphthalimides[19] and anthraquinone (AQ)[16, 20] derivatives have been found to damage DNA by oxidizing its bases.

The Schuster group has been using AQ derivatives to study charge transfer through DNA. The AQ derivatives are either covalently linked at the 5'-end to a DNA strand (figure 4) or are internally linked to the 2'-O position of the sugar moiety of uridine (UAQ).[21] The 5'-linked AQ is attatched to the DNA with a short linker and end caps the DNA duplex while the internally linked AQ intercalates between the base

pairs.[22] Circular dichroism (CD) spectroscopy and 2D-NMR spectroscopy were used to show that the internally linked AQ intercalates between the bases at the 3' side of the uridine.[23, 24]

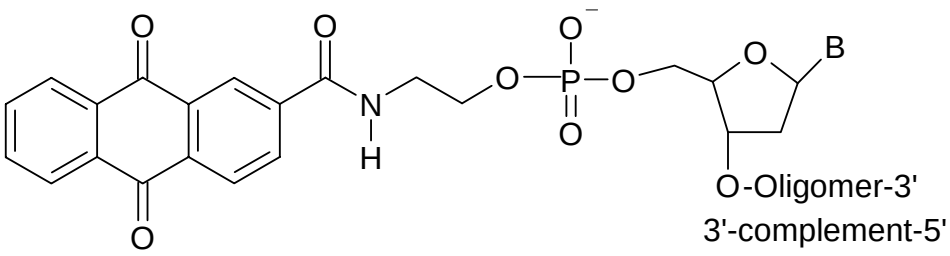

Figure 4. Structure of anthraquinone linked to 5'-end of DNA

As the singlet excited state of AQ is energetic enough to oxidize any of the DNA bases, irradiation of DNA containing AQ leads to electron transfer from its neighboring base which leads to formation of the AQ radical anion and base radical cation. This subsequently leads to charge recombination (back electron transfer or BET) to return AQ to its ground state. Another pathway equally as fast is intersystem crossing (ISC) of the AQ to its triplet excited state which forms a triplet radical ion pair. This triplet excited state like the singlet excited state is energetic enough to oxidize any of the DNA bases. As the triplet radical ion pair is relatively long lived, the AQ radical anion now exists long enough to react with oxygen to give superoxide. The superoxide diffuses away and anthraquinone is restored to its ground state. The net result is an isolated radical cation trapped in DNA. The hole can now hop between base pairs or be quenched by reaction with oxygen or water.

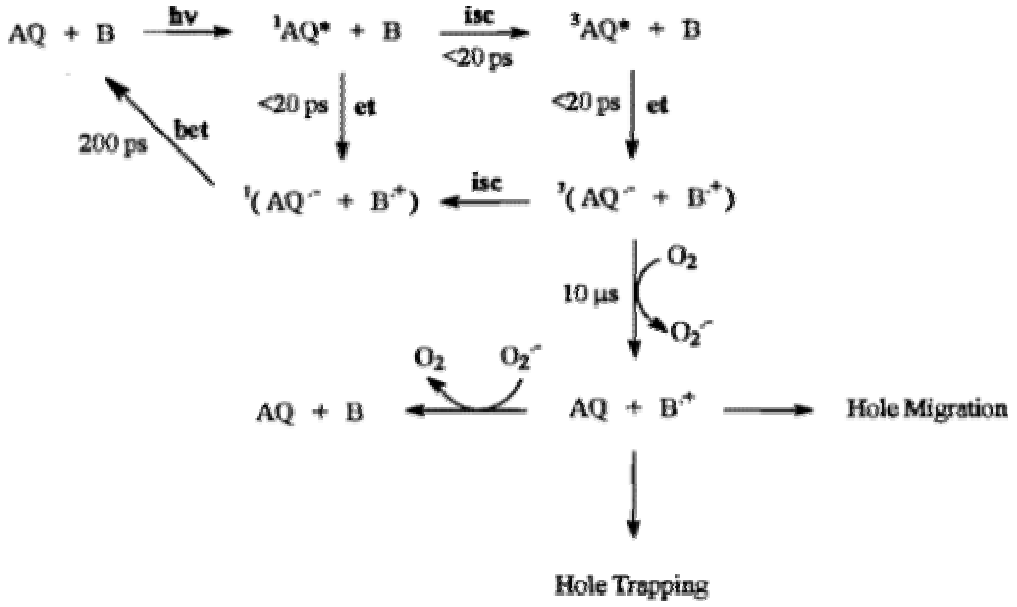

Figure 5. Mechanism of anthraquinone photoexcitation[25]

Methodology

Charge transfer in DNA experiments first require the synthesis and purification of relevant DNA strands. As guanines have the lowest oxidation potential and damage to DNA is concentrated at GG sites, at least one of the DNA strands is designed to contain one to several GG sites along the strand (figure 6). Anthraquinone is usually tethered to one of the single strands at its 5'-end. The strand containing GG steps of interest is ^{32}P radiolabelled at either the 5'-end or the 3'-end (AQ containing strands when necessary, are radiolabeled at the 3'-ends). Following radiolabeling, the DNA strands are hybridized to form duplex DNA. The labeled DNA duplexes are then irradiated at 350nm where only anthraquinone and not DNA absorbs. Optimum irradiation times are chosen in order to maintain single hit conditions.

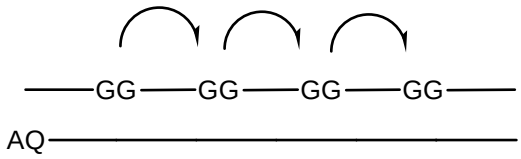

Figure 6. Model for hopping through GG steps

Piperidine treatment of the irradiated DNA leads to DNA strand cleavage at the phosphate backbone of the damaged site. The products are subsequently analyzed via polyacrylamide gel electrophoresis (PAGE) and damage is quantified using a phosphorimager. The efficiency of charge migration can be inferred *via* the extent of damage at GG steps and their proximity to the sensitizer.

As hole migration can be quenched by water,[8, 9] there is always competition between migration (hopping) of the radical cation (k_{hop}) and its reaction with water (k_{trap}). If the rate of hopping is much greater than the rate of trapping (reaction with water), equal amounts of damage will be observed at each GG step. If the reverse were true, damage (if any) should be limited to the first GG step. Many studies have shown charge transport through DNA is not only sequence specific but also distance dependent; that is, the amount of damage at a GG step decreases as a function of its distance from the origin of the radical cation.[6, 7]

Carbazole as potential monitor for charge transfer through DNA

Strand cleavage analysis is an indirect method of looking at charge transfer through DNA and as a consequence, only rough estimates have been made about the rate of hopping of the radical cation.[26] A method to observe charge transfer which does not

rely on reaction with water could prove valuable. Also, as strand cleavage analysis can be a lengthy process, a reliable method of monitoring charge transfer through DNA that doesn't involve radiolabelling, strand scission at GG steps and PAGE analysis is desirable. One way of doing this is to monitor the transient absorption of the guanine radical cation. The difficulty in this is that the guanine radical cation has a very low extinction coefficient and is difficult to observe.

Observation of charge transport in DNA independent of guanine oxidation requires a molecule that will trap the radical cation, and since guanine is the most easily oxidized base, the molecule needs to have a lower oxidation potential than guanine. A suitable molecule that undergoes an observable change (chemical or spectroscopic) upon oxidation can potentially be used to monitor charge transfer through DNA.

Majima and co-workers used the transient absorption spectra of phenothiazine and pyrene derivatives to monitor hole transfer through DNA.[27, 28] Phenothiazine and pyrene are known to intercalate DNA (phenothiazine only partially intercalates) and have lower oxidation potentials than guanine. Their results suggest that hole transfer from a guanine radical cation to phenothiazine takes place in the time scale of 100μs.

In Majima's studies, both the pyrene and phenothiazine are linked to the 5' end of DNA and not intercalated. To truly take the place of guanine, the molecule should ideally be located within the DNA ladder in approximately the same orientation as guanine ie: base stacked. The molecule should also be covalently attached to the DNA strand so that its location relative to the DNA bases is known. It should also be linked to DNA in such a manner that it not only intercalates to DNA but causes little or no disturbance in the stability of the DNA duplex. If this can be achieved, the molecule can

be placed in any position along the DNA strand and can be used to calculate rates of charge transfer in DNA.

A potential molecule for this study is carbazole. Carbazole is a planar compound with an oxidation potential lower than that of guanine[29] and its radical cation has a very high extinction coefficient with an absorption maximum at ~ 800 nm.[30] Carbazole dications are known to intercalate in DNA[31] and although UV-Vis and CD spectra of mixtures of N-methyl carbazole with calf thymus DNA show little or no binding (intercalation or groove) association, it is hoped that once carbazole is covalently linked to the 2' position of a uridine intercalation will occur in a similar manner to AQ when it is linked to uridine. Carbazole (Cz) intercalated in DNA is expected to act as an electron donor to an oxidized oligodeoxynucleotide (ODN) to form its radical cation.

$$\mathbf{Cz\text{-}ODN^{\bullet+} \rightarrow Cz^{\bullet+}\text{-}ODN}$$

Although earlier work has demonstrated the instability of a carbazole radical cation (anodic oxidation leads to formation of a very unstable cation radical that reacts via coupling-deprotonation to 9,9,- and 3,3,-bicarbazyls),[29] it is believed that the intercalated state of the carbazole between DNA base pairs will stabilize the radical cation enough for its observation.[32]

The aim of this project was to first synthesize uridine derivatives with a covalently linked carbazole moiety on the 2' position of the sugar (figure 7). One is attached through the carbazole nitrogen with a 4 carbon linker (U4Z) and the second via a 1 carbon linker through C3 carbon of carbazole (U1Z). The derivatives would be optimized for use in a DNA synthesizer and used to synthesize oligomers which would be

used with a suitable photosensitizer to monitor efficiency of charge migration in DNA sequences containing carbazole.

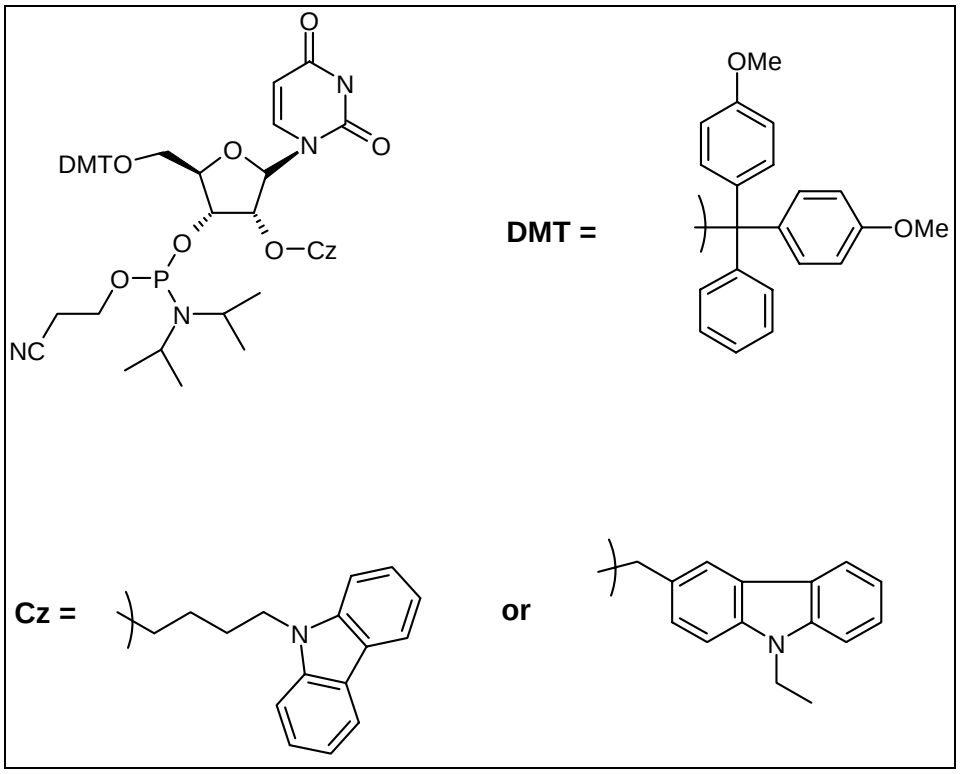

Figure 7. Target compounds – carbazole linked uridines

SYNTHESIS

Four Carbon-Linker Carbazole Uridine (U4Z)

The carbazole uridine phosphoramidite was synthesized using the commercially available starting materials carbazole and uridine. A four carbon linker was attached to the nitrogen of carbazole following a slightly modified version of the Kumanotani[33] procedure (scheme 1). Stirring carbazole with excess 1,4-dibromobutane under basic conditions in the presence of benzyltributylammonium chloride, a phase transfer catalyst (PTC), afforded N-(4'-bromobutyl)carbazole in good yield.

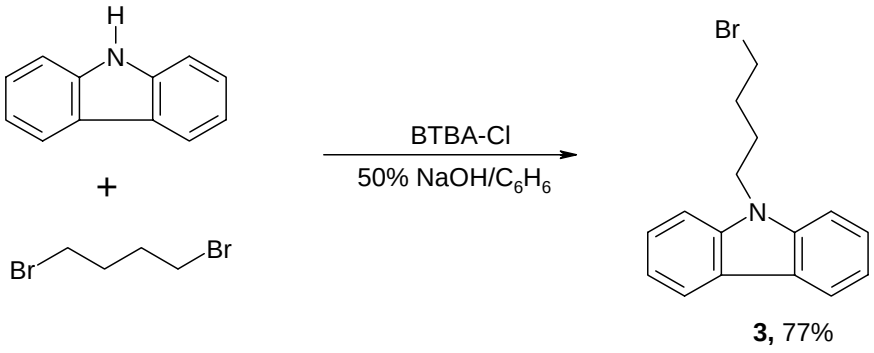

BTBA-Cl = benzyltributylammonium chloride

Scheme 1. Synthesis of bromobutyl carbazole

For the synthesis of 2',3'-O-(dibutylstannylene)uridine, a solution of uridine and dibutyltinoxide in methanol was heated under reflux for one hour. The procedure was published by Moffatt[34] and afforded the desired product in quantitative yield.

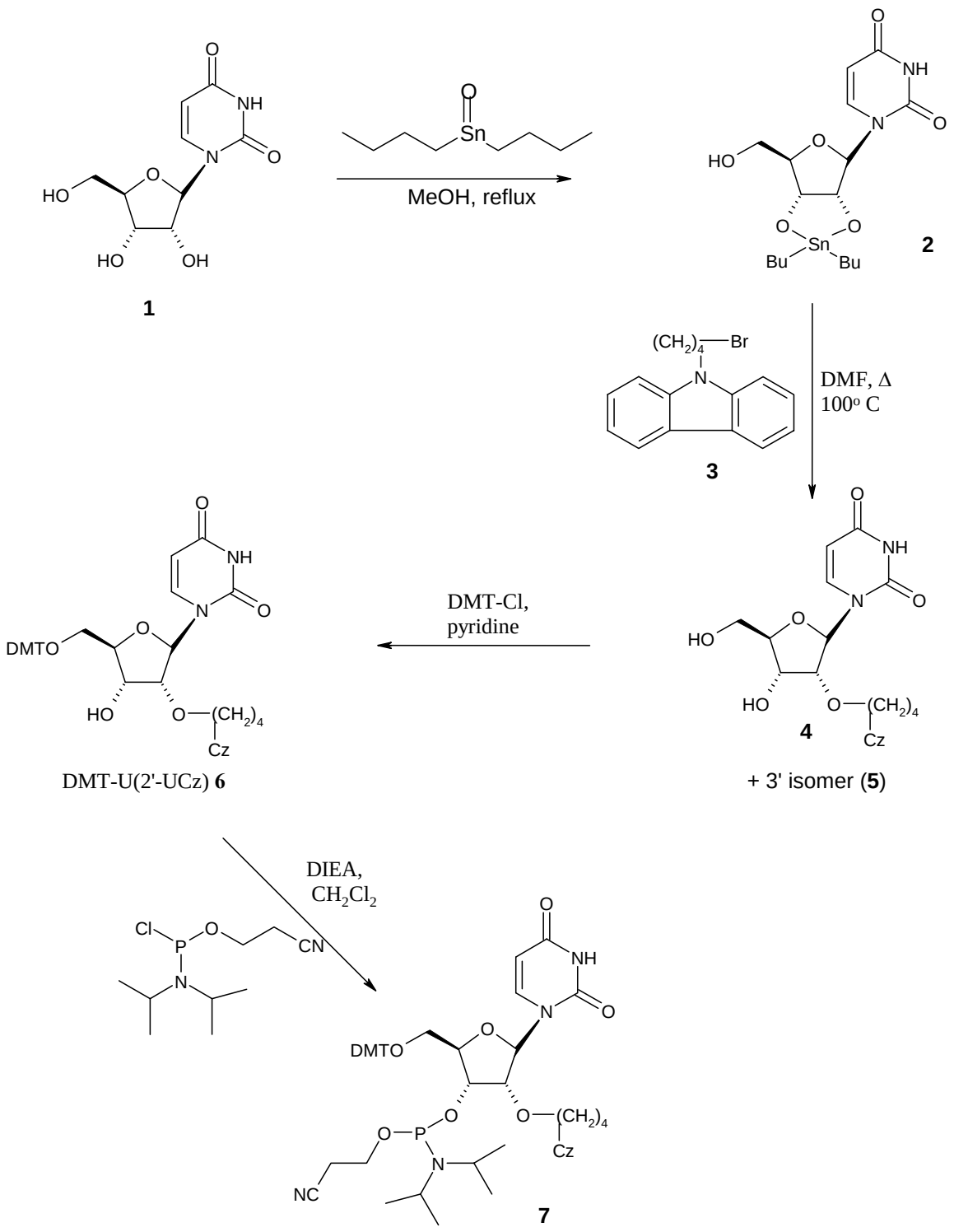

Scheme 2. DMT-U4Z phosphoramidite synthesis

Coupling of carbazole moiety to uridine was achieved by heating 2',3'-O-(dibutylstannylene)uridine and N-(4'-bromobutyl)carbazole in dimethyl formamide (DMF) at 100^{o} C. This reaction led to the monoalkylation of the 2' and 3' oxygens of uridine in fair yield. A mixture of isomers was collected (**4** and **5**). ^{1}H NMR spectra (figure 8) indicated the presence of both isomers in an approximately 50:50 ratio and mass spectral analysis confirmed the correct molecular weight (figure 9).

Dimethoxytrityl (DMT) protection of the 5'-OH group of the ribose proceeded successfully. The two isomers were separated to afford the desired 2' isomer **6**, in high yield. The structure of the correct isomer was confirmed by ^{1}H NMR (figure 10) and 2D-^{1}H NMR analysis (figure 11).

With the correct isomer in hand, a phosphoramidite group was attached to the 3' oxygen of the DMT protected carbazole uridine. This reaction proceeded smoothly and purification afforded pure phosphoramidite in high yield. ^{1}H NMR and ^{31}P NMR spectroscopy confirmed the presence of the phosphoramidite group.

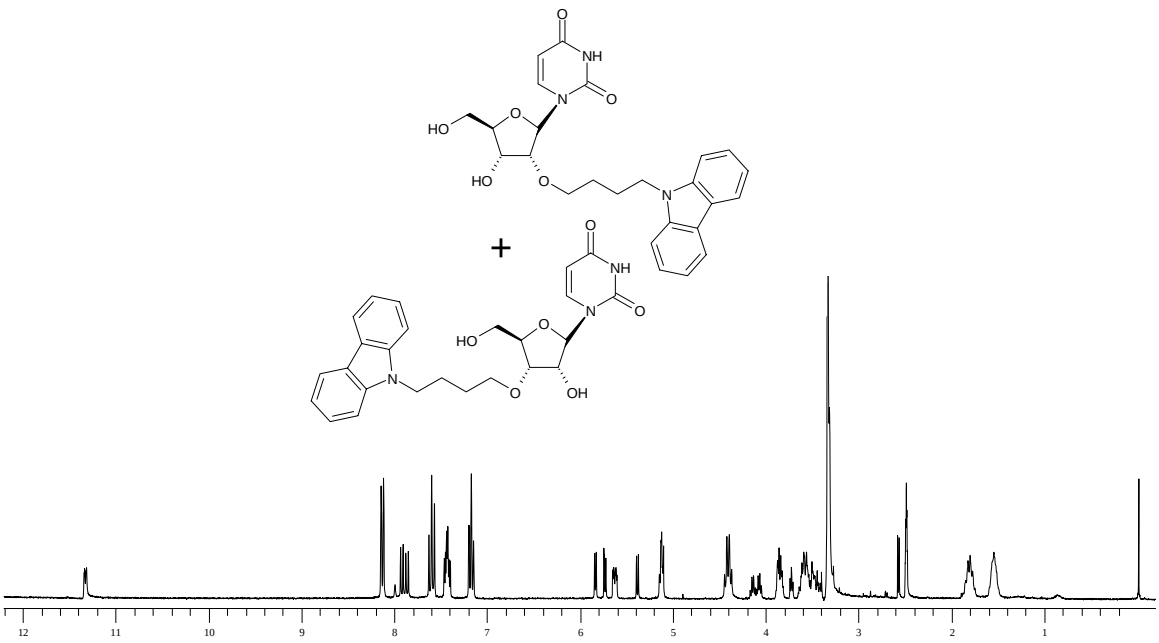

Figure 8. ^{1}H NMR spectrum of both isomers of uridine linked carbazole U4Z **4**, **5**

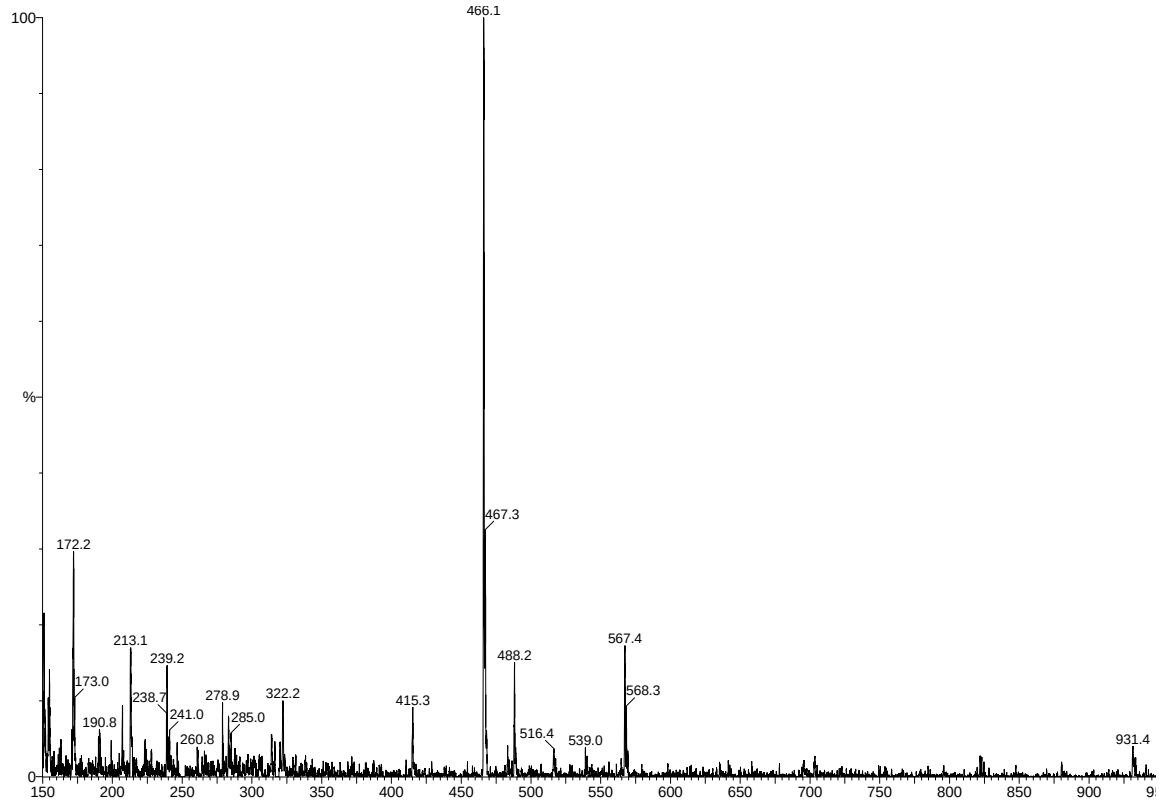

Figure 9. ESI mass spectrum of U4Z, **4**

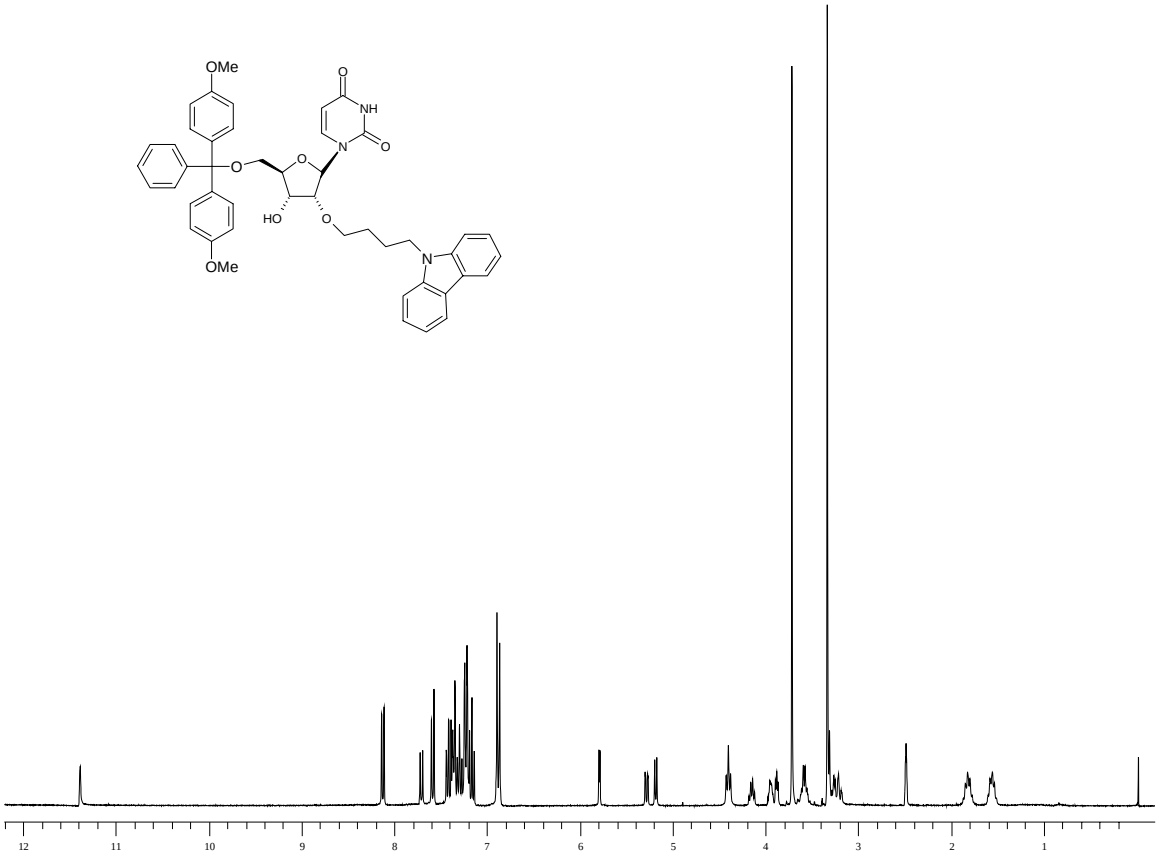

Figure 10. ^{1}H NMR spectrum of DMT-2'O-U4Z, **6**

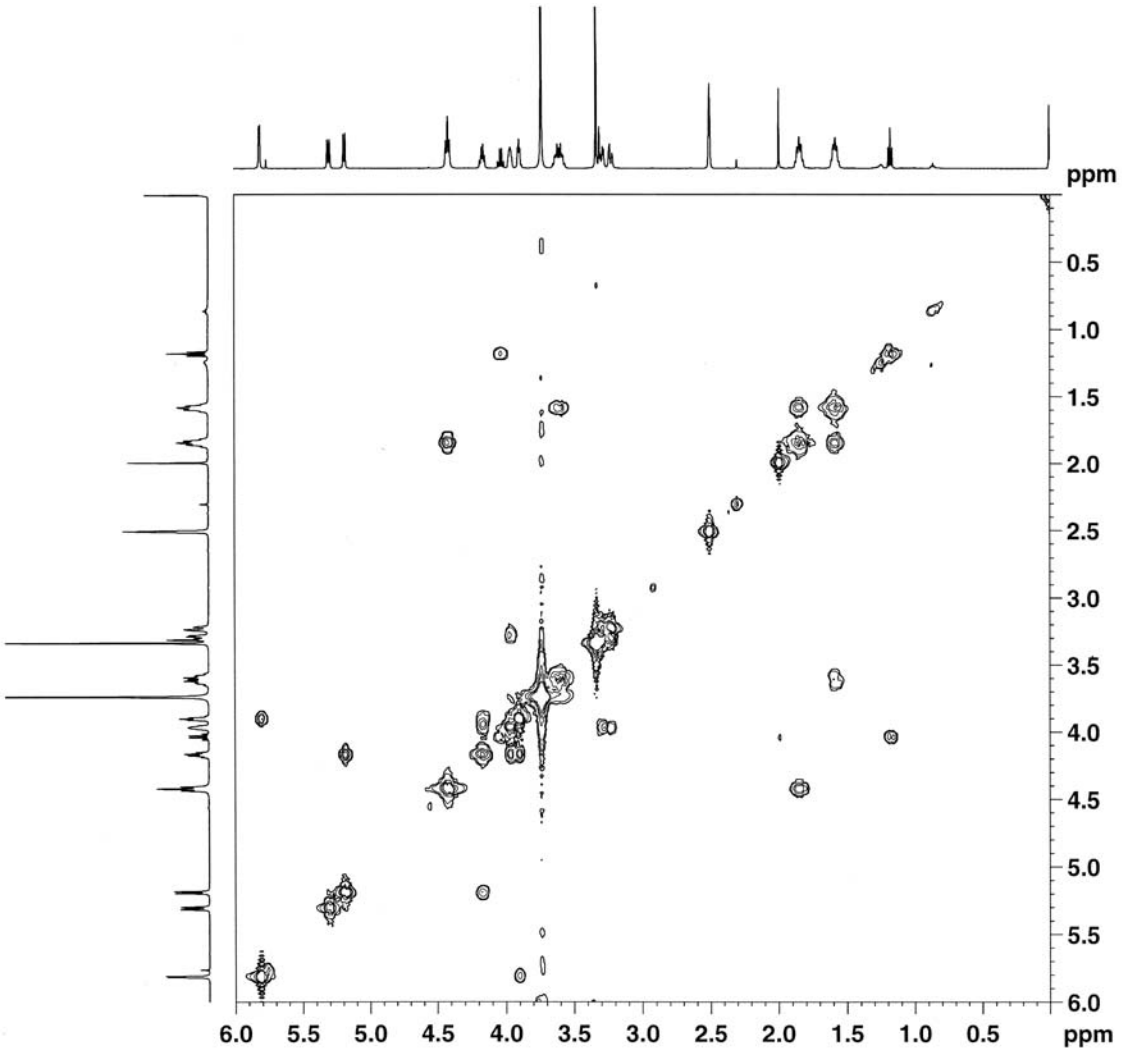

Figure 11. 2D-NMR spectrum of 2'-O isomer of DMT-U4Z, **6**

One Carbon linker Carbazole Uridine (U1Z)

The one carbon linker carbazole uridine (U1Z) was synthesized in a similar manner to U4Z. The 3-bromomethyl-N-ethyl carbazole was synthesized in 2 steps (scheme 3). The first step was reduction of the appropriate N-ethyl carbazole aldehyde to

its corresponding alcohol with sodium borohydride. The second step involved the conversion of the alcohol to its bromide using phosphorus tribromide (PBr_3).

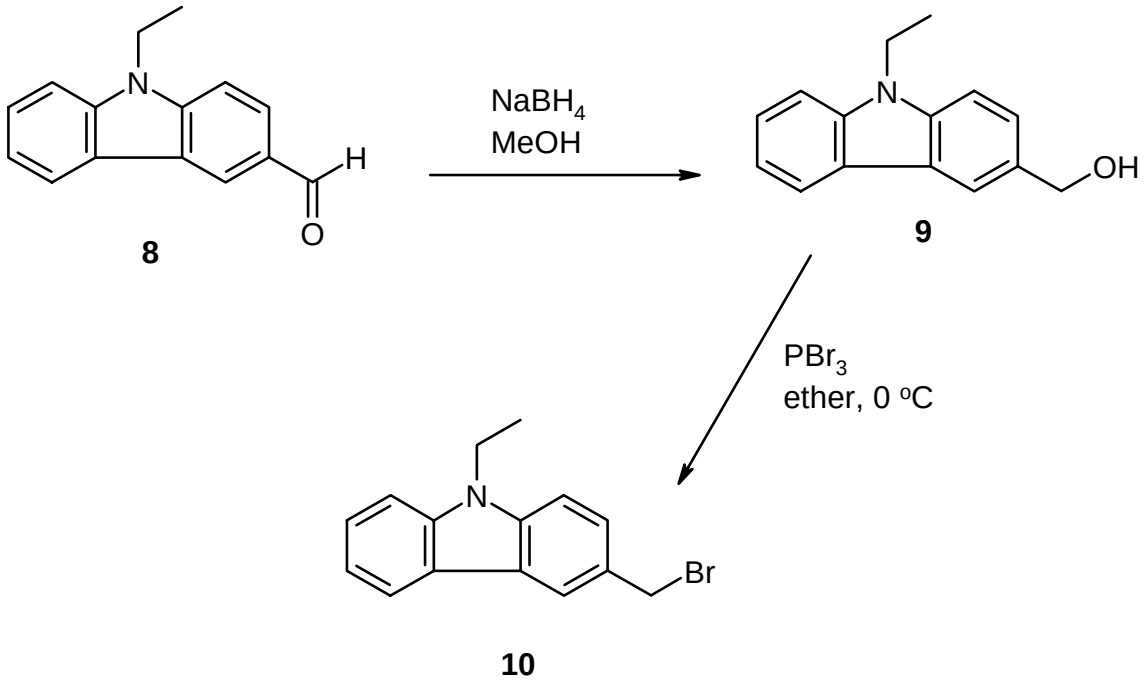

Scheme 3. Synthesis of bromomethyl carbazole

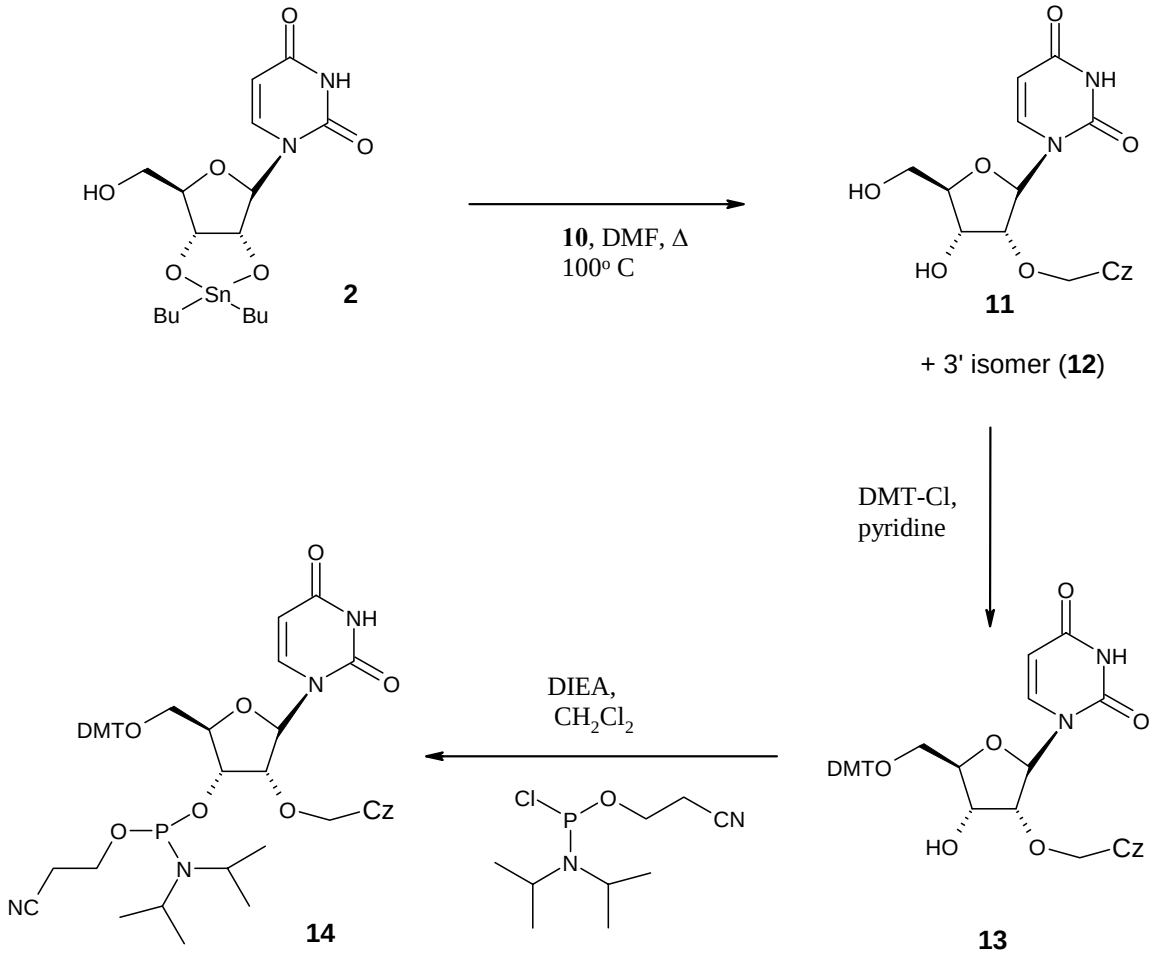

Scheme 4. Synthesis of 1 carbon linker carbazole uridine

The resulting bromide was highly unstable and rapidly decomposed once the work-up solvent (diethyl ether) was removed. As any unreacted alcohol would have little to no effect on the subsequent step of the synthesis (coupling to dibutylstannyleneuridine), the bromide was used without purification. Synthesis of the one carbon linker carbazole followed the same path as that of the four carbon linked uridine (scheme 4).

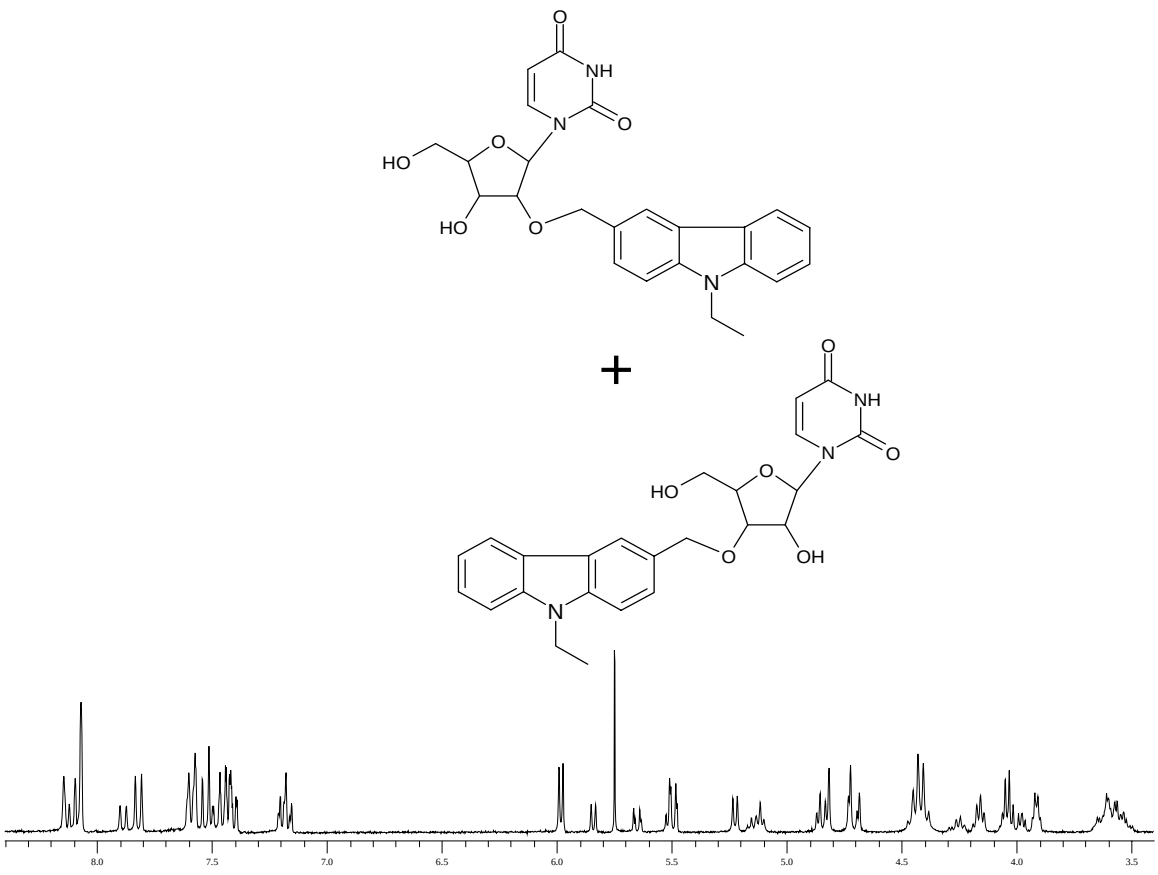

Figure 12. ^{1}H NMR spectrum of both 2’ and 3’ isomers of U1Z (**11**, **12**)

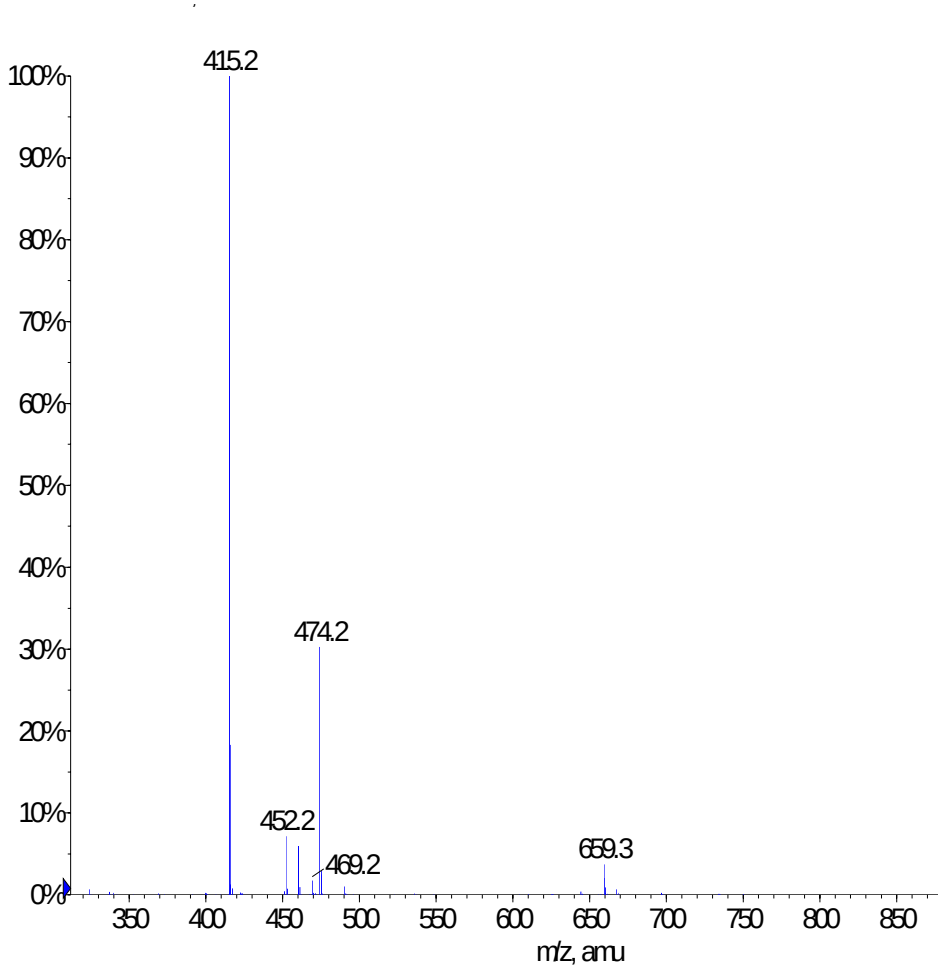

Figure 13. Mass spectrum of 1C linker carbazole uridine, U1Z (**11**)

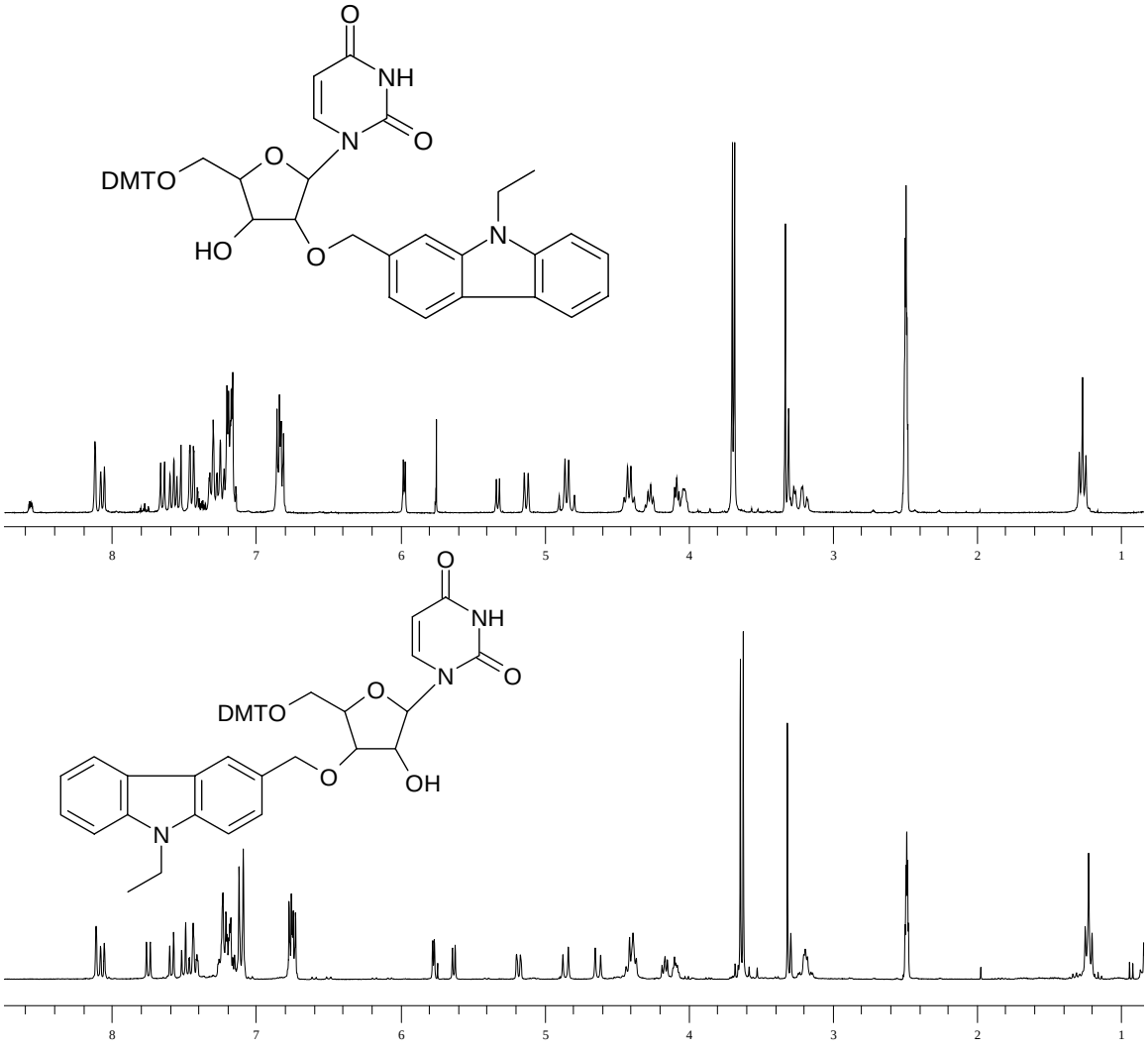

Figure 14. ^{1}H NMR Spectrum of DMT 1C carbazole uridines (desired isomer **14**, top)

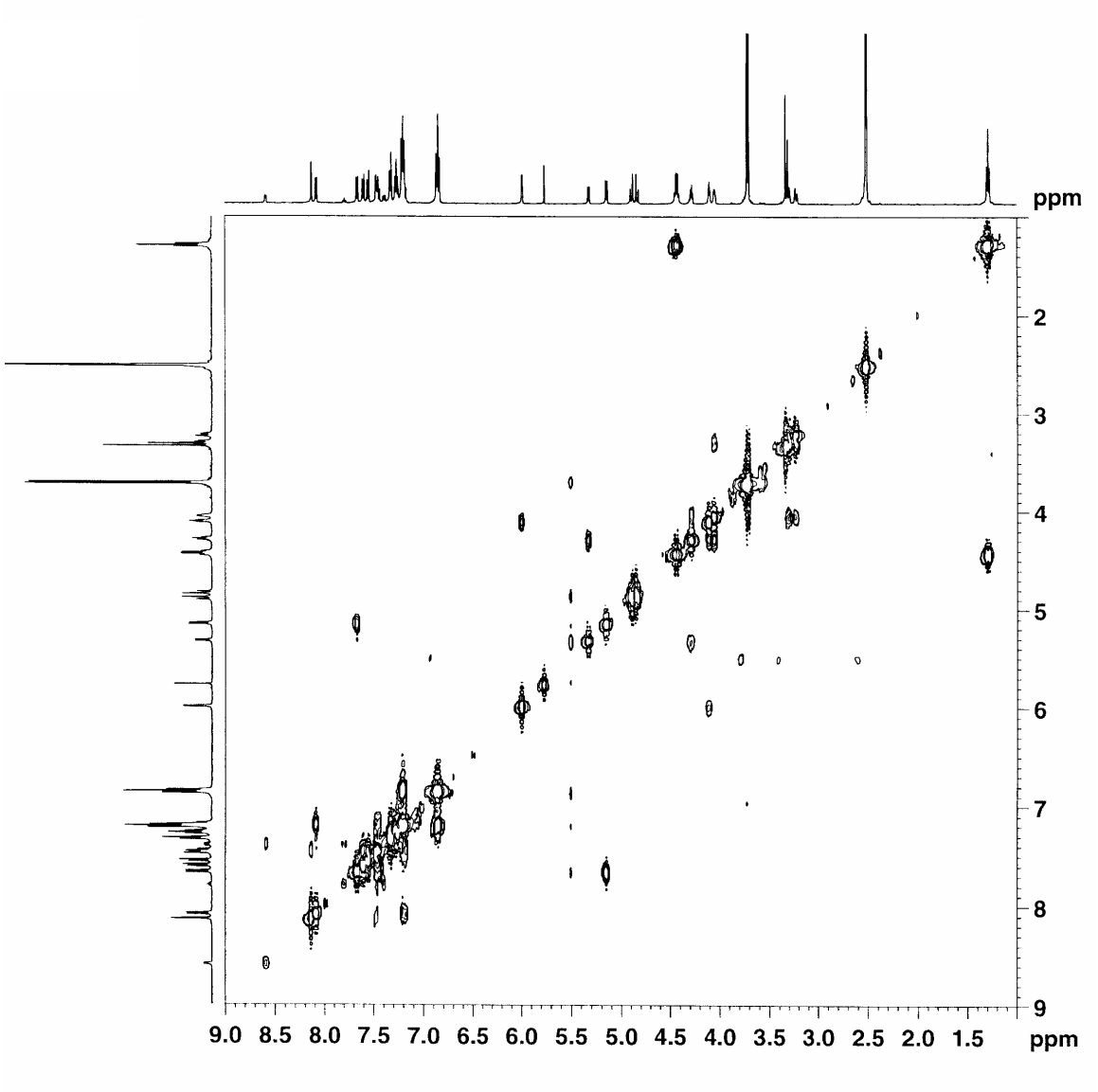

Figure 15. 2D-NMR spectrum of 2'O isomer of DMT-U1Z

The phosphoramidites of both DMT-U4Z and DMT-U1Z (compounds **7** and **14**) were used in making the oligomers CZ1B, Z8, Z12 and Z16 (figure 16). The oligomers are identical in base length (22 bases) and have the same sequence of bases that include

alternating GGs and TTs. The only difference in the oligomers is in the position of the modified uridine. The oligomer CZ1B contains U4Z at the indicated position and the oligomers Z8, Z12 and Z16 all contain the U1Z at the indicated locations. An unmodified oligomer with thymine in place of the modified uridine, N1B and its complementary strand N1A was also synthesized for control experiments. All the DNA strands were purified with HPLC, characterized by UV-Vis spectroscopy and mass spectral analysis. Melting temperature analysis was used to assess duplex formation and carbazole interaction with DNA duplex.

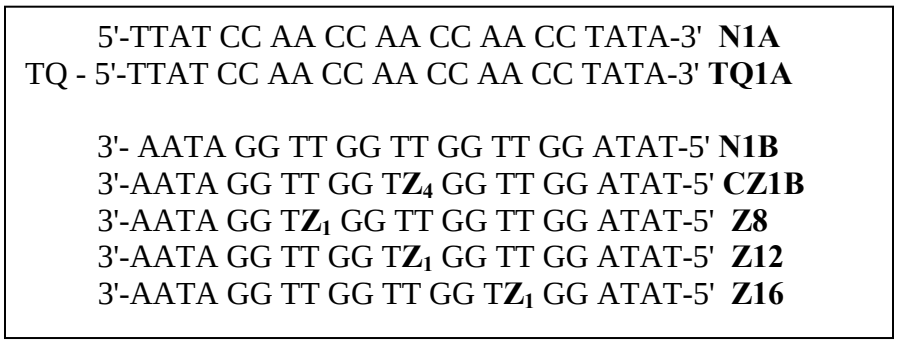

Figure 16. Oligomer sequences used for experimentation

After melting temperature experiments, charge transfer experiments were conducted on the oligomers. As carbazole has a fairly significant UV absorption around 350 nm (where AQ absorbs) the carbazole containing oligomers will need to be annealed to a complementary strand containing a photosensitizer other than AQ. Tetracene quinone (TQ), is a photosensitizer that has been used to oxidize DNA in the same manner as AQ (figure 17).[35] The TQ derivative unlike AQ is irradiated at 420nm. As neither

carbazole nor any of the DNA bases absorb UV light at this wavelength, concurrent irradiation of either carbazole or any of the DNA bases is not expected to occur.

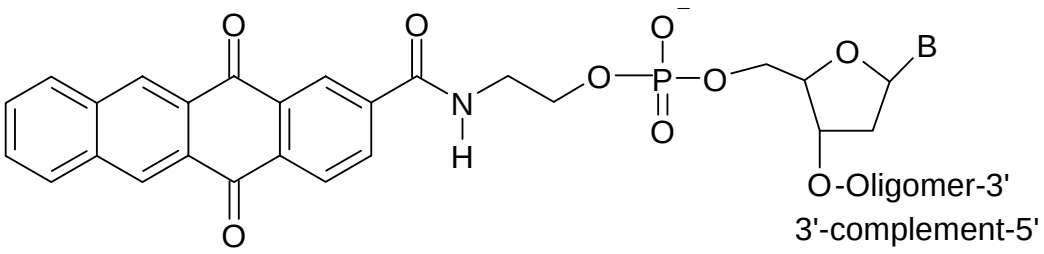

Figure 17. Tetraquinone linked to 5’ end of DNA

The carbazole containing oligomers (CZ1B, Z8, Z12 and Z16) and the unmodified oligomer were hybridized with the complementary TQ containing sequence TQ1A, irradiated and results of the irradiation were assessed via gel electrophoresis and phosphorimagery.

RESULTS AND DISCUSSION

Synthesis

Carbazole was selected for spectroscopic study of charge transfer through DNA because it is a planar molecule that has been shown to intercalate DNA and it has an oxidation potential lower than that of guanine. Also, its radical cation has a very high extinction coefficient with a maximum at ~ 800 nm and should be easy to detect.

Linking a planar molecule to the 2' position of uridine which subsequently intercalates to DNA is something we were quite familiar with in this research group. With that knowledge, linking carbazole to uridine was expected to follow the same steps as linking anthraquinone to uridine (scheme 5). The four carbon linker length was used as a middle ground between the carbazole reaching and intercalating between base pairs on the 3' side of DNA and carbazole hanging in solution or wrapping around or binding to the DNA groove. The one carbon linker moiety U1Z was synthesized because it bore closer resemblance to UAQ which is known to intercalate to DNA than the four carbon linker.

Attempts at coupling bromobutylcarbazole to stannylated N-benzoyluridine failed (scheme 6). The procedure called for stirring a mixture of the compounds in DMF in the presence of cesium fluoride (CsF) for 48 hours. However, after 96 hours, recovered products appeared to be carbazole linked to the 5’-O position and carbazole linked to the N3 position (with concurent debenzoylation). The coupling step was repeated but instead of using CsF to encourage formation of alkoxide ion on the 2' and 3' oxygens, sodium iodide (NaI) was used as a nucleophilic catalyst. This gave the same disappointing results.

The desired coupling of carbazole to uridine could only be achieved by heating both materials in DMF in the absence of CsF.

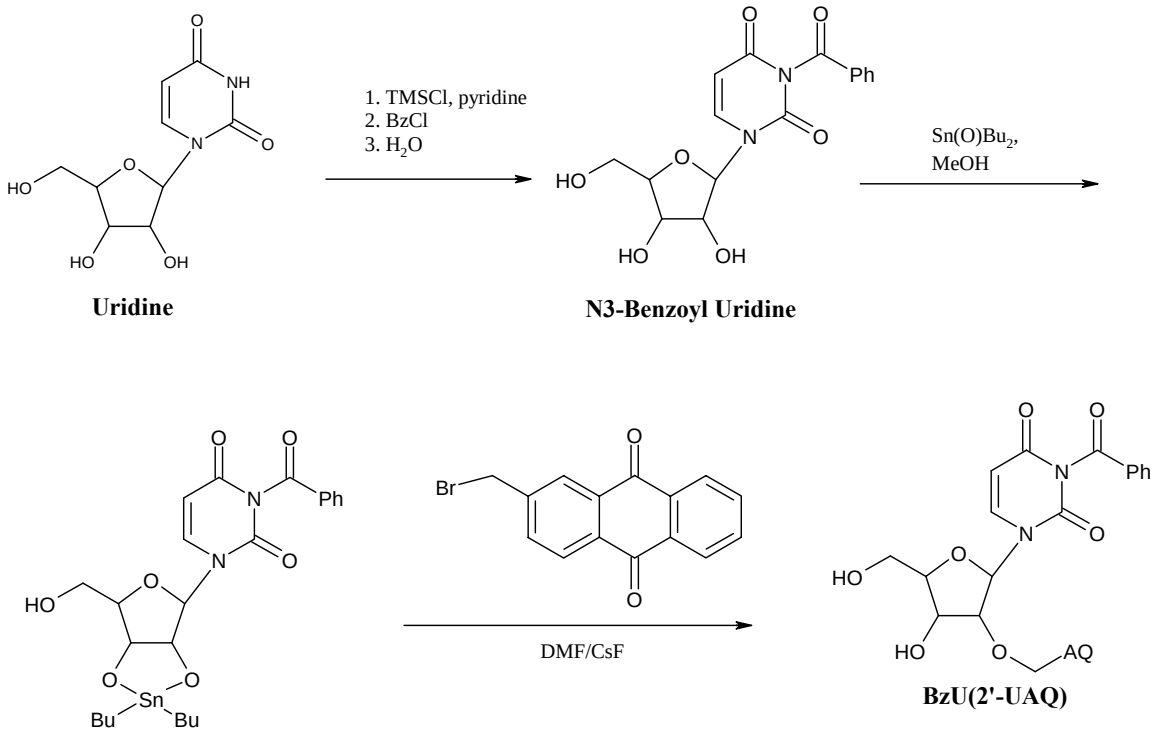

Scheme 5. Synthesis of UAQ[21]

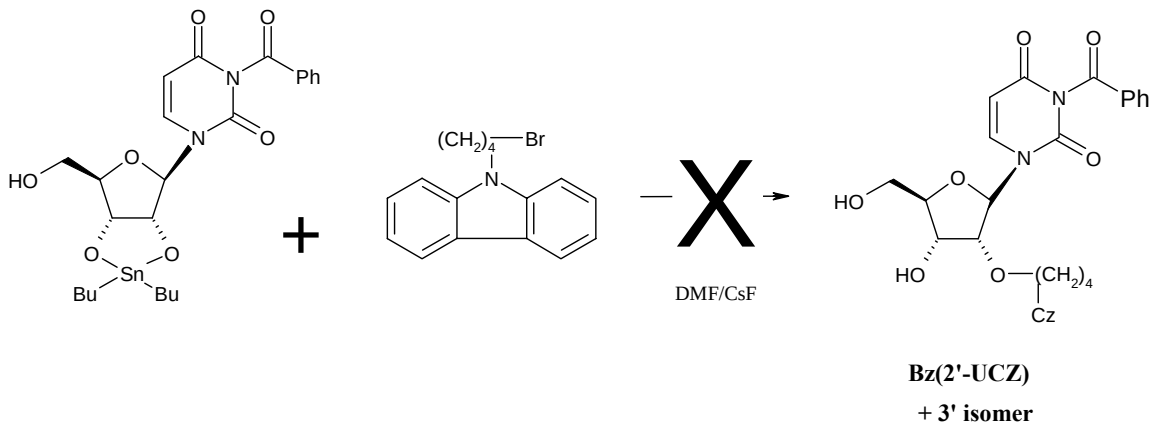

Scheme 6. Failed carbazole coupling step

The reason for the failure of this step is elusive. A number of factors such as poor quality of starting materials or wet solvent may have come into play. These factors however do not seem to have such negative effects on UAQ synthesis.

Both U4Z and U1Z were incorporated into a DNA sequence that was recently used to successfully monitor charge transfer through DNA.[36] The synthetic oligonucleotides were synthesized using standard automated solid-phase DNA synthesis methods. The sequences of the strands prepared are shown in figure 16 where Z_4 stands for U4Z and Z_1 stands for U1Z. The oligomers were cleaved from solid support using standard conditions and purified by HPLC. Their composition and purity were confirmed by HPLC, mass spectrometry and UV-Vis spectroscopy.

The presence of the carbazole moiety in the CZ1B is clearly visible under UV-Vis analysis (see figure 18 and figure 19). The strong absorption at 260nm due to DNA bases and a weaker band at ~ 330 nm due to carbazole can be seen in the spectrum of the oligomer containing carbazole.

The ESI mass spectrum (figures 20, 21) provides highly convincing evidence that carbazole is linked to the DNA. The ESI spectrum yields a sharp peak with *m/e* = 7099 which matches the mass calculated for CZ1B. The ESI mass spectrum of Z8, Z12 and Z16 showed sharp peaks at *m/e* = 7085 which also match the calculated mass.

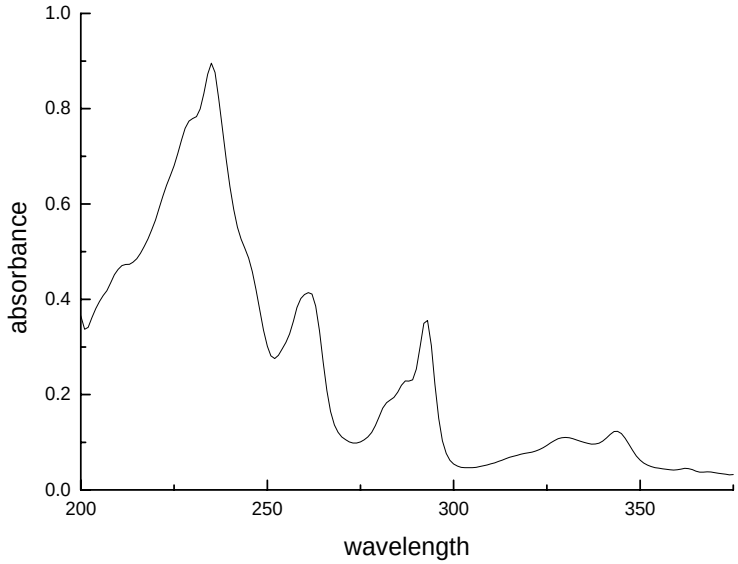

Figure 18. UV-Vis spectrum of N-methylcarbazole in MeOH

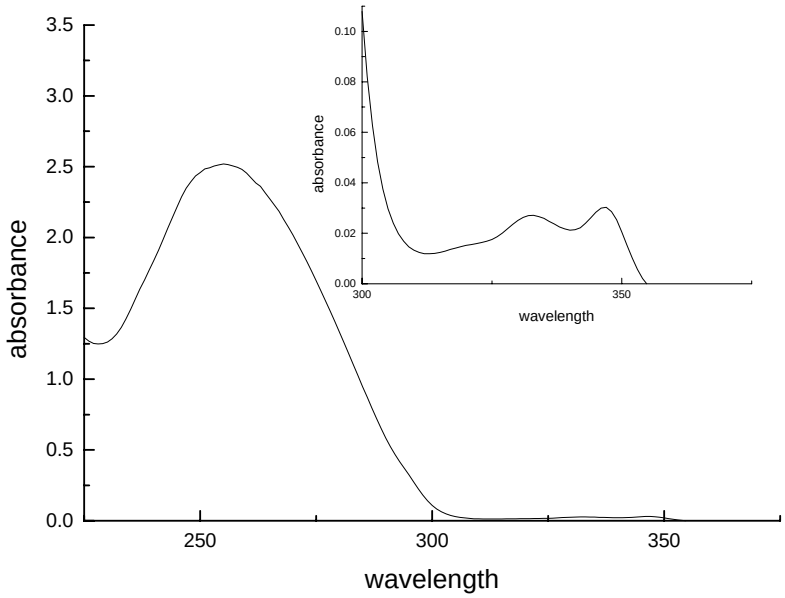

Figure 19. UV-Vis spectrum of CZ1B oligomer

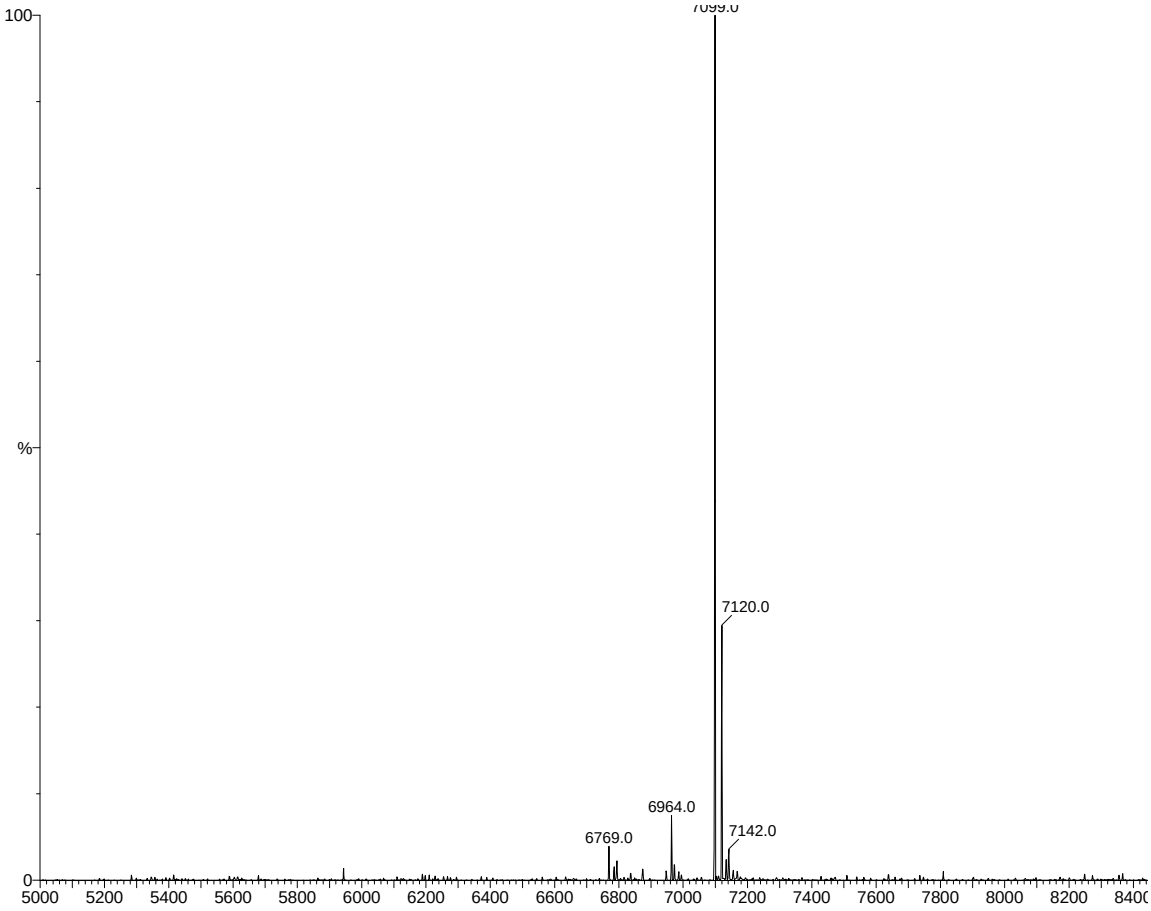

Figure 20. Mass spectrum of CZ1B oligomer

Figure 21. Mass spectrum of Z12 oligomer.

Melting Temperature

We examined the melting behavior of the U4Z and U1Z conjugated duplexes to assess the binding mode of the carbazoles. Figures 22 and 23 show the melting curves for duplexes formed between the oligomers CZ1B, Z8, Z12, Z16 and N1B and their complementary sequence N1A. All the duplexes exhibit monophasic cooperative melting behavior at 260nm where both DNA bases and carbazole absorb. The melting temperature for the carbazole containing duplexes were slightly lower than that of the non carbazole containing duplex (N1B/N1A). The melting transitions when monitored at 330nm where carbazole absorbs but not DNA, show no Tm for the N1B/N1A duplex, a transition around 50 ^{o}C for the CZ1B/N1A duplex and a transition around 45 ^{o}C for the Z8, Z12 and Z16 sequences (figure 23).

Although the Tm study clearly indicates duplex formation for CZ1B/N1A, the results are a little surprising since the carbazole containing strands melt at lower temperatures than the unmodified control duplex. This is surprising because intercalators are known to raise the melting temperature of DNA and not lower it. In fact, the presence of UAQ in DNA causes an increase in its Tm.[23, 21] The fact that the Tm of the carbazole containing oligomers is lower than that of the normal duplex, suggests a possible disruption of base stacking in the duplex. This disruption could be caused by the presence of the alkyl groups in the interior of the DNA interfering with the π-π stacking of the base pairs. The disruption appears more pronounced for the 1C linker oligomers than the 4C linker oligomer.

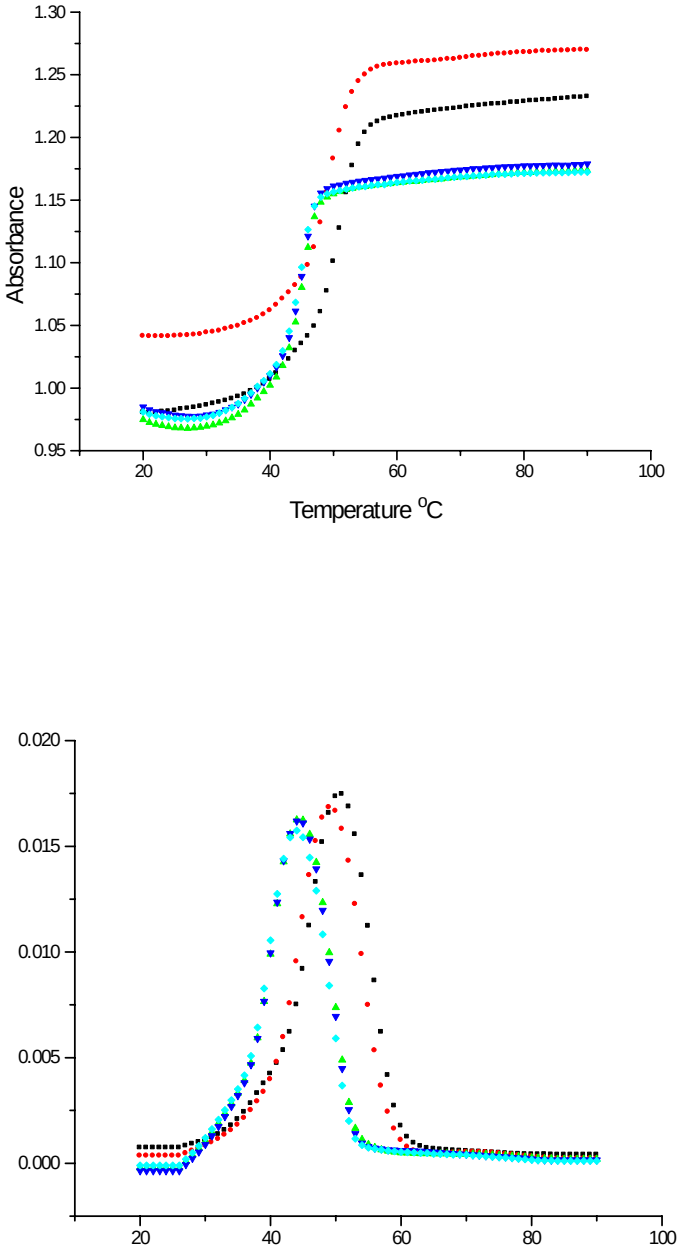

Figure 22. Melting curves for DNA duplexes monitored at 260nm

Thermal denaturation (top) and first derivative (bottom) curves for the DNA duplexes. Melting temperatures are as follows: normal = 51°C, Cz1B = 49 °C, Z8, Z12 and Z16 = 44 °C

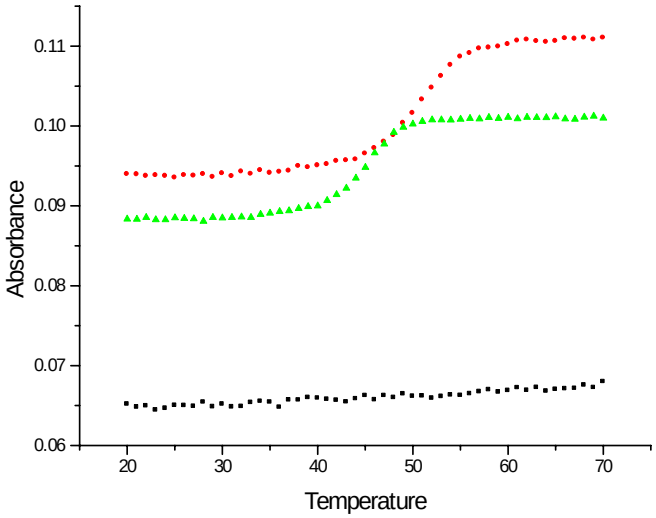

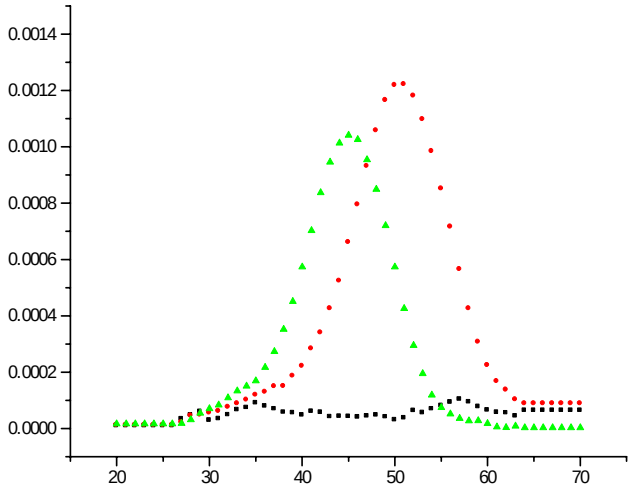

Figure 23. Melting curves for modified duplexes monitored at 330nm

top – Thermal denaturation for Cz1B (red) duplex and Z12 duplex (green) and unmodified duplex (black).
bottom – First derivative curves of melting curves above. Melting temperatures are CZ1B = 50 °C, Z12 = 45 °C, unmodified = no transition

Strand cleavage analysis

After hybridization to the TQ containing complementary strand (TQ1A), the oligomers were irradiated and after treatment with piperidine damage was analyzed by PAGE . The autoradiogram (figure 24) shows equal amounts of damage over the four GG steps for the unmodified strand (N1B). As expected, the 5'G of the GG steps shows a higher susceptibility to damage than the 3'G. The damage pattern for the modified sequences show very little GG damage after the hole encounters the carbazole moiety. This indicates that the carbazole acts as a deeper hole trap than guanine. This is also expected as carbazole is known to have a lower oxidation potential than guanine.

Phosphorimagery was used to quantify the damage at each GG step of all five strands. Figure 25 shows a plot of the damage at the 5'G of each of the four GG steps relative to total damage over all 4 GG steps. The unmodified sequence shows even damage over the four GG steps while the modified sequences (except Z8) show a steep fall off in GG damage after the first GG step. Also GG damage comparison of the 1C linker carbazole uridine (U1Z) to the 4C linker carbazole-uridine (U4Z) indicates no difference in their effectiveness as hole traps.

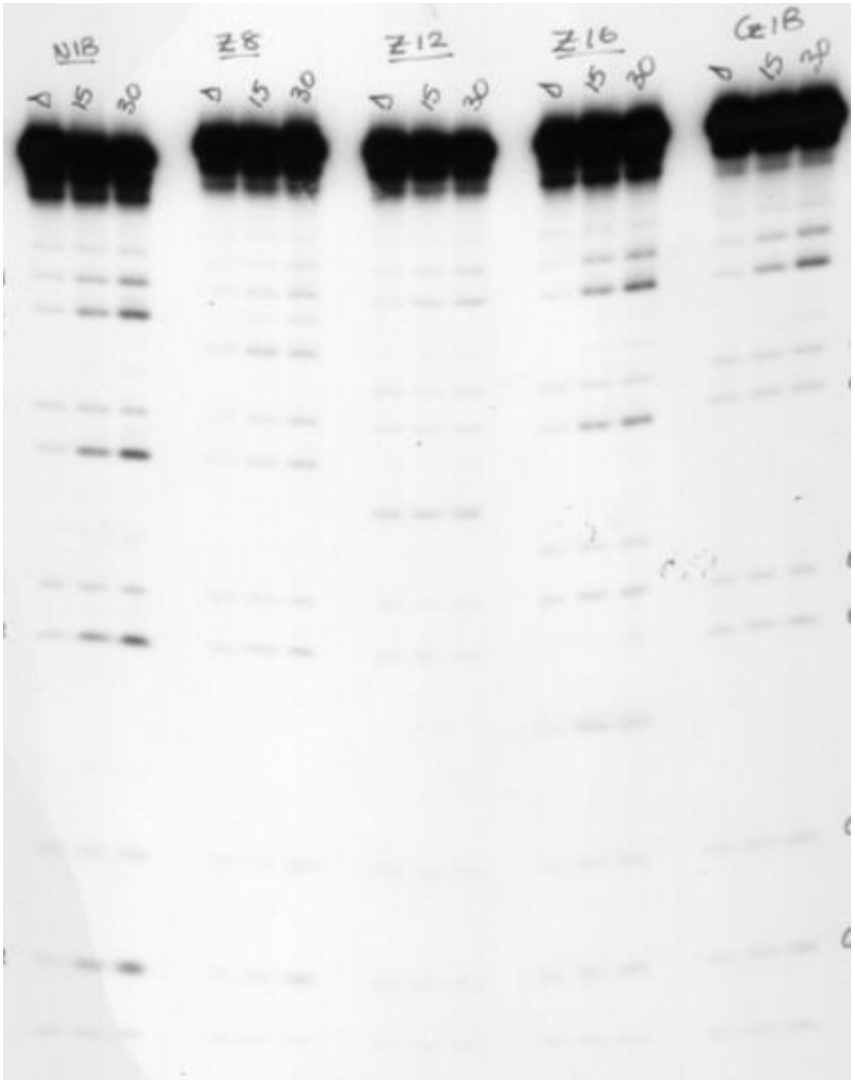

Figure 24. Autoradiogram of a denaturing gel electrophoresis for 5'- 32P-labeled DNA

The first lane in each sample is dark control (D - no irradiation) and the next two lanes are for sequences irradiated for 15 and 30 minutes. All samples were irradiated at 420nm and treated with hot (90 °C) piperidine for 30 min.

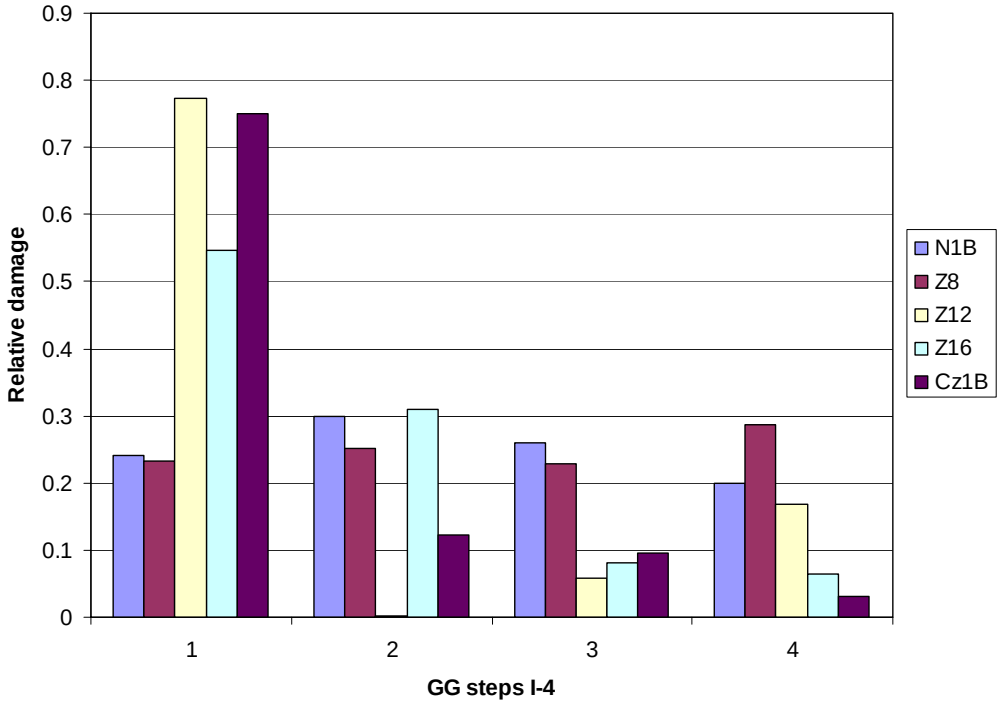

Figure 25. Relative damage on the 5' G of GG steps 1-4.

Relative damage = actual damage/ total damage over the four Gs. Unmodified sequence (blue) indicates even damage through four GG steps. Modified sequences show steep drop after first GG step.

CONCLUSION

Synthesis of carbazole linked uridine was successful and incorporation into DNA was successfully accomplished. The carbazole modified uridines, once incorporated to DNA, form stable duplexes with their complementary strands. This means that this method of internally linking carbazole to DNA causes little disturbance to DNA structure. Strand cleavage analysis confirms that the presence of carbazole within the DNA duplex creates a highly effective hole trap for charge migration.

With this system in hand, further work on DNA charge transfer can be monitored via time resolved absorption spectroscopy.

EXPERIMENTAL

General Methods

1H NMR spectra were recorded on a Varian 300 MHz Spectrometer. Synthetic oligonucleotides were synthesized on an Expedite DNA synthesizer and were, therein, purified by reverse-phase HPLC. Molecular mass of oligonucleotides was determined by electron spray ionization (ESI) mass spectrometry. The extinction coefficients of the oligonucleotides were calculated using nearest-neighbor values and absorbance was measured at 260 nm. UV melting and cooling curves were recorded on a Cary 1E spectrophotometer. The buffer used for all DNA experiments was 10mM sodium phosphate at pH = 7.0.

UV Thermal Denaturation

2.5μM solutions of oligonucleotides and their complementary strands were prepared in 10mM phosphate buffer at pH = 7 and placed in quartz cuvettes (1.5ml capacity, 1cm pathlength). The cuvettes were sealed to prevent evaporation during the heating/cooling cycles. Melting curves were obtained by monitoring UV absorbance of the solutions at 260nm while heating or cooling the solutions between 20-90 °C. The melting temperatures (T_m) were determined as the maxima of the first derivative plot of absorbance versus temperature.

Cleavage Analysis by Radiolabelling and PAGE

DNA oligomers were radiolabelled at the 5'-end using [γ-^{32}P] ATP and T4 Polynucleotide Kinase. The labeling was performed according to standard procedures. Radiolabeled DNA was purified by 20% PAGE. The DNA band was excised from the gel, eluted overnight and ethanol-precipitated in the presence of 1μL glycogen. The samples for irradiation were prepared by hybridizing a mixture of unlabeled DNA ("cold") and radiolabeled oligonucleotide (5μl) with the complementary TQ strand to a total volume of 20μl each in 10mM sodium phosphate, pH = 7.0. The DNA was hybridized by heating the samples at 90 °C for five minutes followed by slowly cooling for several hours. The samples were irradiated in microcentrifuge tubes in a Rayonet photoreactor (Southern New England Ultraviolet Company, Barnsford, CT) equipped with 8 X 420nm lamps. Irradiation times were chosen so that "single hit" conditions were maintained. Irradiation was followed by precipitation with cold ethanol and glycogen followed by washing with 80% ethanol. The samples were then treated with piperidine at 90 °C for 30 minutes to cleave the DNA at the damaged sites. After evaporation of the piperidine the samples were dried, suspended in loading buffer (3000cpm) and electrophoresed on 20% 19:1 acrylamide:bisacrylamide gel containing 7% urea. The gels were dried and cleavage sites visualized by autoradiography.

Synthesis of 4C linker carbazole oligomer

Carbazole, uridine and other reagents for organic synthesis were purchased from Aldrich and Sigma (St. Louis, MO). Starting materials were used without further purification.

Schemes (1) and (2) were followed in the synthesis of carbazole linked uridine.

N-(4-Bromobutyl)carbazole (3) A mixture of carbazole (1g, 6mmol), 1,4-dibromobutane (7.1ml, 60mmol), benzene (3ml), tributylbenzylammonium chloride (-68mg, 0.22 mmols) and 50% NaOH solution was place in a round-bottom flask. The mixture was stirred at 40^{o} C for 1 hour. The solvent was removed under reduced pressure and the crude product was extracted with chloroform. The organic fractions were washed with water and dried over Na_2SO_4. The crude material was purified by column chromatography (silica gel, EtoAc/Hex = 1:3 R_f = 0.6). Yield 1.40g (77%) ^{1}H NMR ($CDCl_3$) δ 1.87-1.98 (m, 2H, Br-$CH_2C\mathbf{H}_2CH_2CH_2$Cbz), 2.02-2.12 (m, 2H, Br-$CH_2CH_2C\mathbf{H}_2CH_2$Cbz), 3.39 (t, 2H, Br-$C\mathbf{H}_2CH_2CH_2CH_2$Cbz), 4.37 (t, 2H, Br-$CH_2CH_2CH_2C\mathbf{H}_2$Cbz), 7.24 (t, 2H, carbazole H3, H6), 7.41 (d, 2H, carbazole H1, H8), 7.47 (t, 2H, carbazole H2, H7), 8.11 (d, 2H, carbazole H4, H5).

2',3'-O-(Dibutylstannylene)uridine (2) The Moffat[34] procedure for stannylation of uridine was followed with no modifications.

2'-O-(N-butylcarbazole)uridine, 3'-O-(N-butylcarbazole)uridine (4, 5) To a solution of 2',3'-O-(Dibutylstannylene)uridine (**2**, 988mg, 20mmol) in DMF, N-(4-Bromobutyl)carbazole (**1,** 1.28g, 40mmol) was added. The mixture was stirred at 100^{o} C for 8 hours. The mixture was allowed to cool and ethyl acetate was added. It was then washed with water and finally dried with Na_2SO_4. The solvent was removed under

reduced pressure and the crude products which show as one spot on TLC ($MeOH/CH_2Cl_2$ = 1:15, R_f = 0.3) was applied to silica gel and eluted with $MeOH/CH_2Cl_2$ = 1:30. The desired product and the 3' isomer were collected without separation. Yield 260mg (28%). ^1H NMR (DMSO–d_6) δ 1.45-1.60 (m, 2H, U3'O-$CH_2C\mathbf{H}_2CH_2CH_2$Cbz), 1.79 (m, 2H, U3'O-$CH_2CH_2C\mathbf{H}_2CH_2$Cbz), 3.40-3.61, 3.72, 3.84, 4.07, 4.14 (H_5, $H_{5'}$, H_4, H_3, H_2 and CH_2O on alkyl chain), 4.41 (-NCH_2 of alkyl chain), 5.12 and 5.38 ($C_{2'}$–OH, $C_{3'}$-OH and $C_{5'}$-OH), 5.62, 5.72, 5.83 (uracil H_5, $H_{1'}$), 7.18 (t, 2H, carbazole H_3, H_6), 7.43 (t, 2H, carbazole H_2, H_7), 7.60 (d, 2H, carbazole H_1, H_8), 7.86, 7.927.18 (t, 2H, carbazole H_3, H_6), 7.43 (t, 2H, carbazole H_2, H_7), 7.60 (d, 2H, carbazole H_1, H_8), 7.72 (d, 1H, uracil H_6), 8.14 (d, 2H, carbazole H_4, H_5) (uracil H_6), 8.14 (d, 2H, carbazole H_4, H_5)

5'-DMT,2'-O-(N-butylcarbazole)uridine(6) The two isomers (**3** and **4**, 232mg, 0.5mmols) and DMT-Cl (338mg, 0.6mmols) were dissolved in dry pyridine (6ml) at room temperature. The mixture was stirred under nitrogen for six hours. The solvent was removed under reduced pressure and mixture was dissolved with a minimum volume of CH_2Cl_2 and applied to a silica gel column. Elution with $MeOH/CH_2Cl_2$ (1:40) gave two major fractions which were separated as 5'DMT-U(2'-CZ) (**5**, 134mg) and 5'DMT-U(3'-CZ) (**6**, 180mg). Total yield 314mg, (82%). ^1H NMR (DMSO–d_6) δ 1.59 (m, 2H, U3'O-$CH_2C\mathbf{H}_2CH_2CH_2$Cbz), 1.84 (m, 2H, U3'O-$CH_2CH_2C\mathbf{H}_2CH_2$Cbz), 3.26 (m, 2H, $H_{5'}$), 3.59 (m, 2H, U3'O-$C\mathbf{H}_2CH_2CH_2CH_2$Cbz), 3.73 (s, 6H, CH_3O of DMT), 3.89 (t, 1H, H_2), 3.96 (m, 1H, H_4), 4.16 (q, 1H, H_3), 4.41 (m, 2H, U3'O-$CH_2CH_2CH_2C\mathbf{H}_2$Cbz), 5.18 (d, 1H, $C_{3'}$-OH), 5.28 (d, 1H, uracil H_5), 5.79 (d, 1H, H_1), 6.88, 7.22 – 7.39 (m, 13H,

DMT), 7.18 (t, 2H, carbazole H_3, H_6), 7.43 (t, 2H, carbazole H_2, H_7), 7.60 (d, 2H, carbazole H_1, H_8), 7.72 (d, 1H, uracil H_6), 8.14 (d, 2H, carbazole H_4, H_5).

5'-DMT,2'-O-(N-butylcarbazole)uridinephosphoramidite(7) DMT-(2'O-UCZ) (**6**, 160mg, 0.21mmols) was dissolved in dry CH_2Cl_2 (2ml) and DIEA (0.2ml, 1.14mmols) was added. The mixture was purged with N_2 and 2-cyanoethyldiisopropylchloro-phosphoramidite (0.10ml, 0.5mmol) was added dropwise. The reaction mixture was stirred at room temperature for 60 minutes then methanol (0.8ml) was added followed by DIEA (0.2ml) in EtOAc (4ml). The mixture was washed with 10% $NaHCO_3$ and dried with Na_2SO_4. The solvent was removed and the mixture was applied to a silica gel column. Elution with CH_2Cl_2/EtOac/Et_3N (45:45:10) gave on major fraction with R_f = 0.7, yield 168mg of white crystals (84%). ^{31}P NMR δ 148.4.

REFERENCES

1. Voet, D.; Voet, J. G. *Biochemistry*, John Wiley & Sons, INC, second ed. New York.

2. Watson, J. D.; Crick, F. H. C. *Nature*, **1953**, *171*, 737

3. Kiefer, J. R.; Mao, C. Braman, J. C.; Beese, L. S. *Nature*, **1998** *391*, 304

4. Weaver, R. *Molecular Biology*, WCB McGraw-Hill, **1999**

5. Demple, B.; Harrison, L. *Annu. Rev. Biochem.* **1994**, *63*, 915-948

6. Henderson, P. T. ; Jones, D.; Hampikian, G.; Kan, Y.; Schuster, G. B. P*roc. Natl. Acad. Sci*. U.S. A **1999**, *96*, 8353-8358

7. Núñez, M. E.; Hall, D. B.; Barton, J. K. *Chem. Biol*. **1999**, *6*, 85

8. Giese, B. *Acc. Chem. Res*. **2000**, *33*, 631

9. Schuster, G. B. *Acc. Chem. Res.* **2000**, *33*, 253.

10. Steenken, S.; Jovanovic, S. V. *J. Am. Chem. Soc.* **1997**, *119*, 617.

11. Jovanovich, S. V.; Smimic, M. G. *J. Phys. Chem*. **1986**, *90*, 974

12. Budowsky, E. I; Kovlsky, O. I.; Yakovlev, D. Y.; Simukova, N. A.; Rubin, L. B. *FEBS Lett.* **1985**, *188*, 155

13. Murphy, C. J.; Arkin, M. R.; Jenkins, Y.; Ghatlia, N. D.; Bossman, S. H.; Turro, N. J.; Barton, J. K. *Science* **1993**, *262*, 1025-1029

14. Turro, N. J.; Barton, J. K. *J. Biol. Inorg. Chem.* **1998**, *3*, 201-209.

15. Fahlman, R. P.; Sharma, R. D.; Sen, D. *J. Am. Chem. Soc.* **2002**, *124*, 12477-12485.

16. Ly, D.; Kan, Y.; Armitage, B.; Schuster, G. B. *J. Am. Chem. Soc.* **1996**, *118*, 8747-8748.

17. Kendrick, T.; Giese, B. *Chem. Commun.*, **2002**, 2016-2017

18. Homlin, R. E.; Barton, J. K. *Inorg Chem.* **1995**, *34*, 7-8

19. Saito, I; Takayama, M.; Sugiyama, H.; Nakatani, K.; Tsuchida, A.; Yamamoto, M. *J. Am. Chem. Soc.* **1995**, *117*, 6406-6407.

20. Armitage, B. A.; Yu, C.; Devadoss, C. Schuster, G. B. *J. Am. Chem. Soc.* **1994**, *116*, 9847

21. Ly, D.; Sannii, L.; Schuster, G. B. *J. Am Chem. Soc.* **1997**, *119*, 12762-12771.

22. Gasper, S. M.; Schuster, G. B. *J. Am. Chem. Soc.* **1997**, *119*, 12762-12771.

23. Yamana, K.; Nishijima, Y.; Ikeda, T.; Gokota, T.; Ozaki, H.; Nakano, H.; Sangen, O.; Shimidzu, T. *Bioconjugate Chem.* **1990**, *1*, 319-324

24. Deshmukh, H.; Joglekar, S. P.; Broom, A. D. *Bioconjugate Chem.* **1995**, *6*, 578-586

25. Armitage, B. *Chem. Rev*. **1998**, 98, 1188

26. Voityuk, A. A.; Poesch, N. *J. Phys Chem B* **2002**, *106*, 3013-3018.

27. Kawai, K.; Takada, T.; Tojo, S.; Majima, T. *Tetrahedron Lett*. **2002**, *43*, 89-91.

28. Kawai, K.; Takada, T.; Tojo, S.; Ichinose, N.; Majima, T. *J. Am. Chem. Soc*. **2001**, *123*, 12688-12689.

29. Ambrose, J. F.; Carpenter, L. L.; Nelson, R. F, J. Electrochem. Soc. **1975**, *122*, 876

30. Tadamasa S. *Electronic absorption spectra of radical ions*, Elsevier, **1988**, New York

31. Tanious F A; Wilson W D; Patrick D A; Tidwell R R; Colson P; Houssier C; Tardy C; Bailly C. *Eur. J. Biochem*. **2001**, *268*, 3455-3464

32. Stolze, K.; Mason, R. P, *Chem. Biol. Interact.* **1991**, *77*, 283-9

33. Oshima, R.; Wada, T.; Kumanotani, J. *J. Polym. Sci. Polym. Chem. Ed.* **1984**, *22*, 3135

34. Wagner, D.; Verheyden, J. P. H.; Moffatt, J. G. *J. Org. Chem.* **1974**, *39*, 24

35. Roberts, L. R.; Schuster, G. B. "*The synthesis of a tetracene quinine phosphoramidite photosensitizer to study charge migration through DNA*" **2001**

36. Liu, Chu-Sheng; Schuster, Gary B. *J. Am Chem. Soc*. **2003**, *125*, 6098-6102.